

LATTICE DYNAMICS OF III-V COMPOUNDS

by

Ranjan Banerjee

Submitted in partial fulfillment
of the requirements for the degree of
Master of Science.

Department of Physics,
Faculty of Pure and Applied Science,
The University of Ottawa,
Ottawa, Canada

1967

ABSTRACT

In the present thesis, we have investigated the lattice dynamics of the following III-V compounds: gallium arsenide, gallium phosphide, indium antimonide, indium phosphide and aluminium antimonide on the basis of both second neighbour ionic model and shell model of Kaplan and Sullivan. Results have been presented for the dispersion curves, vibration spectra and Debye temperatures of the above mentioned compounds. The two models have also been compared in the light of these results.

ACKNOWLEDGEMENTS

I wish to express my indebtedness to Dr. Y.P. Varshni for his continuous counsel and suggestion of this problem; the staff of the Computing Centre, for making available time on the IBM 360; Mrs. Louise Carrière for typing the thesis; Dr. R.C. Shukla and Mr. R.C. Blanchard for helpful discussions; and Mr. S. Bose for his encouragement during the tenure of this work.

TABLE OF CONTENTS

| | |
|---|------|
| ABSTRACT..... | iii |
| ACKNOWLEDGEMENTS..... | iv |
| LIST OF ILLUSTRATIONS..... | vii |
| LIST OF TABLES..... | viii |
| CHAPTER I Introduction | 1 |
| CHAPTER II The Secular Equation for the Second Neighbour Ionic Model of the Zinc Blende Lattice | 10 |
| A) Mechanical part | 11 |
| 1. General harmonic lattice vibration theory | 11 |
| 2. Structure and geometry of zinc blende type lattice | 14 |
| 3. Dynamical matrices and elastic constants | 18 |
| B) Coulomb part | 25 |
| 4. Dynamical matrices and elastic constants for SNI model | 29 |
| CHAPTER III Kaplan and Sullivan's Model | 32 |
| CHAPTER IV The Secular Equations for the Special Directions | 39 |
| CHAPTER V The Determination of Parameters | 46 |
| CHAPTER VI Numerical Results and Calculations | 52 |
| 1. Dispersion curves | 57 |
| 2. Frequency spectra | 68 |
| 3. Obtaining Debye Θ curve | 78 |

| | | |
|--------------|---|-----|
| CHAPTER VII | Discussion | 84 |
| | 1. Gallium Arsenide | 87 |
| | 2. Indium Antimonide | 88 |
| | 3. Aluminium Antimonide | 90 |
| | 4. Indium Phosphide | 90 |
| | 5. Gallium Phosphide | 91 |
| APPENDIX I | | 94 |
| APPENDIX II | Diagonalization of 6 x 6 matrix | 95 |
| APPENDIX III | 1. Kellerman Coefficients | 103 |
| | 2. Calculations for SNI Model and KS Model | 103 |
| REFERENCES | | 106 |

LIST OF ILLUSTRATIONS

| | | |
|--------------------------------|---|----|
| Figure (2.1) | Zinc blende lattice | 15 |
| (3.1) | Shell model | 32 |
| The dispersion curves for | | |
| (6.1) | Gallium Arsenide in $[\xi 00]$ direction | 58 |
| (6.2) | Gallium Arsenide in $[\xi \xi \xi]$ direction | 59 |
| (6.3) | Indium Antimonide in $[\xi 00]$ direction | 60 |
| (6.4) | Indium Antimonide in $[\xi \xi \xi]$ direction | 61 |
| (6.5) | Aluminium Antimonide in $[\xi 00]$ direction | 62 |
| (6.6) | Aluminium Antimonide in $[\xi \xi \xi]$ direction | 63 |
| (6.7) | Indium Phosphide in $[\xi 00]$ direction | 64 |
| (6.8) | Indium Phosphide in $[\xi \xi \xi]$ direction | 65 |
| (6.9) | Gallium Phosphide in $[\xi 00]$ direction | 66 |
| (6.10) | Gallium Phosphide in $[\xi \xi \xi]$ direction | 67 |
| The Histograms for SNI model | | |
| (6.11) | Gallium Arsenide | 70 |
| (6.13) | Indium Antimonide | 72 |
| (6.15) | Aluminium Antimonide | 74 |
| (6.17) | Indium Phosphide | 76 |
| (6.18) | Gallium Phosphide | 77 |
| The Histograms for KS model | | |
| (6.12) | Gallium Arsenide | 71 |
| (6.14) | Indium Antimonide | 73 |
| (6.16) | Aluminium Antimonide | 75 |
| The $\epsilon_D(T)$ curves for | | |
| (6.19) | Gallium Arsenide | 79 |
| (6.20) | Indium Antimonide | 80 |
| (6.21) | Aluminium Antimonide | 81 |
| (6.22) | Indium Phosphide | 82 |
| (6.23) | Gallium Phosphide | 83 |

LIST OF TABLES

| | | |
|-----------|--|----|
| TABLE I | Elastic Constant Data | 53 |
| TABLE II | Zone Boundary Frequencies of Different Compounds | 54 |
| TABLE III | Parameters for SNI Model | 55 |
| TABLE IV | Parameters for KS Model | 56 |

CHAPTER I

INTRODUCTION

Semiconductor Physics owes its origin to the characteristic conduction properties of germanium and silicon. In recent years, the properties of a number of other semiconducting substances have been investigated. These other semiconducting substances mainly consist of III-V, II-VI and I-VII group compounds. The importance of the III-V group compounds was first demonstrated by Welker^{1, 2}. He showed that apart from having semiconducting properties they have very close relationship to the semiconductors of the fourth group elements. Actually, his observations of the new important characteristics proved to be a link between germanium, silicon and compounds of II-VI and I-VII groups and it is possible to know the main properties of III-V compounds from those of neighbouring substances.

A good amount of work has been done on the band structure; optical, electric and galvanometric properties of III-V compounds. However, relatively speaking, lattice dynamics and thermal properties of these compounds have received less attention. Insufficiency of available data and the suitable

choice of a theoretical model can be assigned to be the reason³.

A majority of III-V compounds crystallize in zinc-blende lattice, which is similar to the diamond lattice for a monatomic substance.

In 1912, Born and von Karman⁴ published a theory of lattice dynamics for central force interactions between the nearest neighbours. A 2-constant theory involving radial and non-central forces between the nearest neighbours in crystals of diamond type lattice was given by Born (1914)⁵. The elastic constants in this kind of interaction satisfy closely an identity

$$4 c_{11} (c_{11} - c_{44}) = (c_{11} + c_{12})^2 \quad (1.1)$$

where c_{11} , c_{44} and c_{12} are the three principal elastic constants. This is a necessary though not a sufficient condition if the first neighbours are important.

A 3-constant theory was given next by Smith⁶ and by Nagendranath⁷ independently, which took into account a central force interaction between the second nearest neighbours in addition to the central and angular force interactions between the first

nearest neighbours. Smith's theory was applied to germanium and silicon by Hsieh⁸ (corrected by Dayal and Singh⁹). Hsieh's calculations nevertheless failed to account for the experimental results particularly for the frequencies of transverse acoustic modes of short wave length limits where the discrepancy amounts to 70%. It has been shown by Brockhouse and Iyengar¹⁰ (1959) that it is not sufficient to introduce the second neighbour interactions to explain the experimental results on dispersion curves of germanium. Herman¹¹ and Pope¹² showed that it is necessary to use a five neighbour model to fit the dispersion curves of germanium. Braunstein, Moore and Herman¹³ considered a force model in which they considered all the forces for the nearest neighbours and only the angular force for the second nearest neighbours. They applied this model - Angular force model to germanium and found that the frequencies in the Brillouin zone boundaries can be obtained within a good limit of approximation. But they did not calculate the phonon dispersion curves and Debye Θ . It should be noted that in this model, the model of Smith, the second neighbour force constants μ and ν are taken

to be equal.

The Shell model originated by Dick and Overhauser¹⁴, and developed by Cochran^{15, 16} and Cowley¹⁷, and largely equivalent Distortion dipole formulation by Tolpygo^{18, 19} and his group have led to more realistic treatment of the lattice dynamics of these substances.

Cochran regarded each atom as composed of a core of charge Z coupled to an oppositely charged shell by means of an isotropic spring of constant k . He assumes four types of nearest neighbour interactions - core-core, core-shell, shell-core and shell-shell interactions. To keep his model as simple as possible Cochran considered only two force constants to be assigned for each type. One is associated with radial force and the other with the angular force. The formulation of dipoles by the lattice wave gives rise to electro-static forces throughout the crystal. This interaction includes all neighbours and requires no extra parameter. This model has been used with considerable success to account for the dispersion curves and specific heats of diamond (Dolling and Cowley²⁰, Blanchard and Varshni²¹),

silicon (Dolling²²) and germanium (Dolling²²).

So far, we have considered mainly the lattice dynamics of the monatomic substances having lattice structure like that of diamond. A majority of III-V compounds crystallize in the zinc blende lattice. For investigating the lattice dynamics of these compounds one must realize that the bonding is not purely covalent, but belongs to a certain intermediate type between covalent and ionic, thus the ionic contribution to the lattice vibration in these compounds should not be overlooked (Potter²³, Sirota and Gololobov²⁴).

For ionic lattices, Kellermann²⁵ (1941) has shown that the long range coulomb forces contribute a major part in the interaction. Expressions for the coupling coefficients due to the coulomb forces in the equations of motion were given by him. The numerical results shown by Kellermann were on NaCl lattice but they can be easily converted for diamond and zinc blende lattice in a way suggested by Cochran¹⁵.

Merten²⁶ (1958) and Srinivasan and Rajagopal²⁷ (1959) gave theories on the lattice vibration of zinc blende structure

in which they included both the short range forces attributed to covalent bonding and the long range coulomb forces for the ionic part. Their results were not in satisfactory agreement with the experimental values. One of the reasons may be their assumption that the second neighbour forces are central and that Zinc-Zinc and Sulphur-Sulphur interactions are equivalent.

These compounds do not satisfy Born's equation and Born's ratio

$$\frac{4 c_{11} (c_{11} - c_{44})}{(c_{11} + c_{12})^2} \quad (1.2)$$

deviates from unity as can be seen from Table I on page 53.

Thus it is well understood that a simple central force model will not be sufficient to explain the lattice dynamics of these compounds.

The next simple model that can be considered is one similar to Braunstein, Moore and Herman's model for germanium. Attempts were made with this model on III-V compounds but it was found to be unsatisfactory.

Tolpygo and his group²⁸ tried to explain the lattice vibrations in such crystals with the distortion dipole model but he needed more parameters than the experimental data available to him.

Kaplan and Sullivan²⁹ simplified the model of Cochran in the light of Tolpygo's work and also used similar parameters. They considered the core-core, shell-shell and core-shell interactions similar to the rigid ion interaction and for which expressions similar to Smith can be found. They have calculated the frequencies in [100] directions for gallium arsenide, indium antimonide and aluminium antimonide.

Recently, on a similar model Dowling and Cowley²⁰ (1966) have calculated the thermodynamic properties of gallium arsenide and compared them with experimental results. They were able to obtain a very good fit for the dispersion curves. This model involves a large number of parameters and can be successfully applied only to those compounds whose dispersion curves have been measured. Amongst III-V compounds, dispersion curves have been measured only for gallium arsenide³⁰.

In the present thesis, we have investigated the lattice dynamics of GaAs, GaP, InSb, InP and AlSb, firstly on a second neighbour ionic model (SNI model) and then on Kaplan and Sullivan's model (KS model). SNI model is a general force constant model with the force constant matrices for first neighbours as

$$\begin{bmatrix} \alpha & \beta & \beta \\ \beta & \alpha & \beta \\ \beta & \beta & \alpha \end{bmatrix} \quad (1.3)$$

and for the second neighbours as

$$\begin{bmatrix} \lambda_i & \delta_i & \delta_i \\ -\delta_i & \mu_i & \nu_i \\ -\delta_i & \nu_i & \mu_i \end{bmatrix} \quad i = 1, 2 \quad (1.4)$$

We have taken the two parameters μ and ν to be equal in concurrence with the central force model of Smith and angular force model of Braunstein, Moore and Herman. The long-range coulomb forces are also taken into consideration in view of the ionic bonding present in III-V compounds. This model has only a limited number of parameters which can be determined from elastic constant and infra red data. Thus it is possible to apply this model to those substances for whom dispersion curve

measurements are lacking but zone boundary frequencies are known from infra-red measurements. Results are presented for the dispersion curves, vibration spectra and Debye temperatures.

Next, we consider the model of Kaplan and Sullivan.

After a few necessary changes we calculated the thermodynamic properties as before on the basis of the parameters : given in their paper. We assumed Z to be zero when choosing a particular set of parameters from the different sets given - mainly for the simplicity in computation. Comparisons of the results obtained from SNI model and KS model with experimental results are also made.

CHAPTER II

THE SECULAR EQUATION FOR THE SECOND NEIGHBOUR IONIC
MODEL OF THE ZINC BLENDE LATTICE

We shall divide the interaction in two parts

- A) Mechanical part
- B) Coulomb part

As we have said already, the binding in the case of III-V compounds is of a certain type intermediate between covalent and ionic. The mechanical part is due to the covalent bond and Coulomb part is for the ionic.

We shall now derive the MECHANICAL PART of the secular equation:

1. General Harmonic Lattice Vibration Theory

Born and Begbie³¹ developed a general force treatment and it was applied by Smith to diamond lattice and considerably improved by Merten when applying to zinc blende structure. We would briefly describe the formulation.

Let us consider a general lattice structure in which there are n particles to each cell. Distinguishing different particles in the same cell by index $\kappa = 1, \dots, n$ and taking any cell as the reference, we label different cells by l (l^1, l^2, l^3). Thus a particle in general lattice can be specified by l and κ .

If we represent the total potential energy Φ of a lattice as a function of the displacements of the lattice particles from their positions of equilibrium, we can form its derivatives with respect to the component of the particle displacement $u_\alpha \left(\begin{smallmatrix} l \\ \kappa \end{smallmatrix} \right)$. (α -component of the displacement vector of particle $\left(\begin{smallmatrix} l \\ \kappa \end{smallmatrix} \right)$, $\alpha = 1, 2, 3$). Small vibrations of a lattice are controlled by the second neighbours:

$$\left(\frac{\partial^2 \Phi}{\partial u_{\alpha}(\frac{1}{\kappa}) \partial u_{\beta}(\frac{1'}{\kappa})} \right)_0 = \Phi_{\kappa\kappa'}^{(1-1')} \quad (2.1)$$

The symbol on the right is due to the fact that the second derivative depends only on the relative cell index $1 - 1'$ and not on 1 and $1'$ individually. Denoting the position vector of a lattice particle $(\frac{1}{\kappa})$ in the equilibrium configuration by $\vec{r}(\frac{1}{\kappa})$, the complex solutions of the equations of motion are of the form:

$$u(\frac{1}{\kappa}) = v(\kappa) \exp(2\pi i \vec{q} \cdot \vec{r}(\frac{1}{\kappa}) - i\omega t) \quad (2.2)$$

where $v(\kappa)$ is a constant vector depending only on κ . \vec{q} is the wave vector in the reciprocal space. For a given \vec{q} the circular frequency $\omega = 2\pi\nu$ is determined by the following secular equation:

$$\left| M_{\alpha\beta} \left(\vec{q} \right)_{\kappa\kappa'} - \omega^2 \delta_{\kappa\kappa'} \delta_{\alpha\beta} \right| = 0 \quad (2.3)$$

where

$$M_{\alpha\beta} \left(\vec{q} \right)_{\kappa\kappa'} = \frac{1}{\sqrt{m_{\kappa} m_{\kappa'}}} \sum \Phi_{\alpha\beta} \left(\frac{1}{\kappa\kappa'} \right) \exp \left\{ -2\pi i \vec{q} \cdot [\vec{r}(\frac{1}{\kappa}) - \vec{r}(\frac{1'}{\kappa})] \right\} \quad (2.4)$$

the summation being over all integral values of $1^1, 1^2, 1^3$ and m_{κ} and $m_{\kappa'}$ being the particle masses, $\delta_{\kappa\kappa'}$ and $\delta_{\alpha\beta}$ signify Kronecker

delta, e.g.

$$\delta_{ij} = \begin{cases} 1 & \text{if } i = j \\ 0 & \text{if } i \neq j \end{cases} \quad (2.5)$$

Equation (2.3) is a $3n$ degree equation in ω^2 . Restricting ourselves to positive roots only we will find that three of these roots - the acoustic branches - tend to zero as $\vec{q} \rightarrow 0$ and the remaining $3n - 3$ roots - the optical branches, tend to finite limits as $\vec{q} \rightarrow 0$ the first order Raman spectrum of the lattice (not all values of \vec{q} correspond to mutually distinct solutions as shown by Born³² (1923) the choice of the possible wave vectors should be restricted by "cyclic lattice condition").

The elements of the matrix $\Phi_{\alpha\beta} \begin{pmatrix} 1 & -1 \\ k & k' \end{pmatrix}$ are related through the symmetry of the lattice in the following way:

A symmetry operation of the lattice can be expressed as a transformation matrix T , and if $\begin{pmatrix} L \\ K \end{pmatrix}$ is some other lattice point

$$\vec{r} \begin{pmatrix} L \\ K \end{pmatrix} = T \vec{r} \begin{pmatrix} 1 \\ 1 \end{pmatrix} \quad (2.6)$$

The elements will then have the transformation law

$$\Phi \begin{pmatrix} L & -L' \\ KK' \end{pmatrix} = \tilde{T} \Phi \begin{pmatrix} 1 & -1' \\ KK' \end{pmatrix} T \quad (2.7)$$

where \tilde{T} is the transpose of T and the change of indices $\begin{pmatrix} 1 \\ K \end{pmatrix}$ is obtained from equation (2.6).

2. STRUCTURE AND GEOMETRY OF ZINC BLENDE TYPE LATTICE

The III-V compounds whose lattice vibrations we are investigating crystallize in zinc blende lattice. In this kind of lattice each of the two types of ions occupy the sites of a face-centered cubic lattice, the cube side having a length $2a$. The second such lattice is displaced along the body diagonal of the first lattice by one quarter of the cube diagonal ($\frac{\sqrt{3}}{2} a$). The three basis vectors that define the rhombohedral parallelepiped unit cell are

$$\begin{aligned} \mathbf{a}_1 &= a (0, 1, 1) \\ \mathbf{a}_2 &= a (1, 0, 1) \\ \mathbf{a}_3 &= a (1, 1, 0) \end{aligned} \quad (2.8)$$

and thus the volume of the unit cell is $2a^3$.

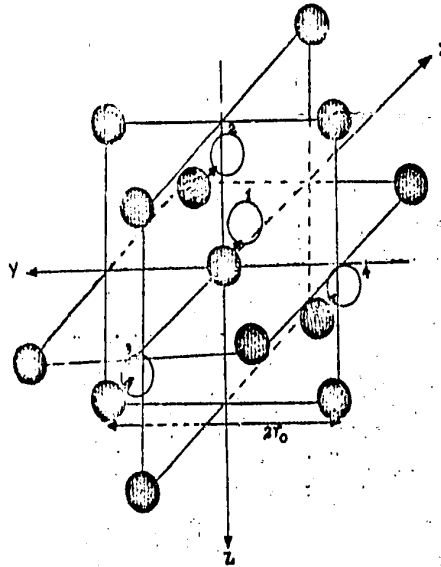


Figure 2.1: Structure of zinc blende lattice

Figure (2.1) represents the lattice structure of zinc blende. The black circle represents the atoms of type I and lattice I and white circles represent the four nearest neighbours of and are in lattice II.

The atoms of lattice I are located by the vector

$$r_I(n) = [(n_1 + n_3) e_1 + (n_1 + n_2) e_2 + (n_2 + n_3) e_3] \quad (2.9)$$

The quantities n_1, n_2, n_3 are integers and e_1, e_2 and e_3 are unit vectors parallel to x, y and z axes respectively.

Lattice II is said to be generated by displacing first lattice through a displacement $\mathbf{r}_{1, 2}$

$$\mathbf{r}_{1, 2} = -\frac{a}{2} (\mathbf{e}_1 + \mathbf{e}_2 + \mathbf{e}_3) \quad (2.10)$$

(the negative sign is chosen in conformity to Cochran and Kellermann).

Thus the location of the atoms in lattice II is given by

$$\mathbf{r}_{II} (n) = \mathbf{r}_I (n) + \mathbf{r}_{1, 2} \quad (2.11)$$

$$= [(n_1 + n_3 - \frac{1}{2}) \mathbf{e}_1 + (n_1 + n_2 - \frac{1}{2}) \mathbf{e}_2 + (n_2 + n_3 - \frac{1}{2}) \mathbf{e}_3] a \quad (2.12)$$

The transformation laws in this lattice can be summarized by the following matrices:

1. Threefold axis of rotation:

$$T_1 = \begin{bmatrix} 0 & 1 & 0 \\ 0 & 0 & 1 \\ 1 & 0 & 0 \end{bmatrix} \quad (2.13a)$$

2. Planes of reflection:

$$T_2 = \begin{bmatrix} 0 & 1 & 0 \\ 1 & 0 & 0 \\ 0 & 0 & 1 \end{bmatrix} \quad (2.13b)$$

3. Rotation through $\frac{\pi}{2}$ about an axis through the point $(\frac{a}{2}, \frac{a}{2}, \frac{a}{2})$ parallel to x_3 -axis followed by a rotation through $\frac{\pi}{2}$ about an axis through the same point parallel to the x_1 -axis:

$$T_3 = \begin{bmatrix} 0 & -1 & 0 \\ 0 & 0 & -1 \\ 1 & 0 & 0 \end{bmatrix} \quad (2.13c)$$

4. Rotation through $\frac{\pi}{2}$ about an axis parallel to the x_1 -axis through the point $(\frac{a}{2}, \frac{a}{2}, \frac{a}{2})$ followed by a rotation through $\frac{\pi}{2}$ about an axis through the same point parallel to the x_2 -axis:

$$T_4 = \begin{bmatrix} 0 & 1 & 0 \\ 0 & 0 & -1 \\ -1 & 0 & 0 \end{bmatrix} \quad (2.13d)$$

5. Rotation through $\frac{\pi}{2}$ about an axis parallel to the x_2 -axis through the point $(\frac{a}{2}, \frac{a}{2}, \frac{a}{2})$ followed by a rotation through $\frac{\pi}{2}$

about an axis through the same point parallel to the x_3 -axis:

$$T_5 = \begin{bmatrix} 0 & -1 & 0 \\ 0 & 0 & 1 \\ -1 & 0 & 0 \end{bmatrix} \quad (2.13e)$$

3. DYNAMICAL MATRICES AND ELASTIC CONSTANTS (MECHANICAL PART)

If we apply the transformations (eq. 2.13) on the force constant matrices we can show that they should be of the form given in expressions (1.3) and (1.4) of Chapter I for nearest and next nearest neighbours of two types respectively*.

The elements of the dynamical matrix in the reciprocal space can be given as (in q_x, q_y, q_z space):

* Herman has pointed out an error in Smith's treatment of next nearest neighbour force constants. The error amounts to the neglect of the parameter δ , which is, in general, non-zero. This was due to an error in the choice of the transformation matrices.

$$\begin{aligned}
 M_{xx} \begin{pmatrix} \vec{q} \\ \kappa\kappa \end{pmatrix} &= \frac{4}{m_\kappa} [\alpha_\kappa + \lambda_\kappa \{1 - \cos \pi q_y \cos \pi q_z\} \\
 &\quad + \mu_\kappa \{2 - \cos \pi q_x \cos \pi q_y - \cos \pi q_x \cos \pi q_z\}] \\
 M_{yy} \begin{pmatrix} \vec{q} \\ \kappa\kappa \end{pmatrix} &= \frac{4}{m_\kappa} [\alpha_\kappa + \lambda_\kappa \{1 - \cos \pi q_z \cos \pi q_x\} \\
 &\quad + \mu_\kappa \{2 - \cos \pi q_y \cos \pi q_z - \cos \pi q_y \cos \pi q_x\}] \\
 M_{zz} \begin{pmatrix} \vec{q} \\ \kappa\kappa \end{pmatrix} &= \frac{4}{m_\kappa} [\alpha_\kappa + \lambda_\kappa \{1 - \cos \pi q_x \cos \pi q_y\} \\
 &\quad + \mu_\kappa \{2 - \cos \pi q_z \cos \pi q_x - \cos \pi q_z \cos \pi q_y\}]
 \end{aligned}
 \tag{2.14}$$

$$\begin{aligned}
 M_{xy} \begin{pmatrix} \vec{q} \\ \kappa\kappa \end{pmatrix} &= \frac{4}{m_\kappa} [\nu_\kappa \sin \pi q_x \sin \pi q_y] = M_{yx} \begin{pmatrix} \vec{q} \\ \kappa\kappa \end{pmatrix} \\
 M_{yz} \begin{pmatrix} \vec{q} \\ \kappa\kappa \end{pmatrix} &= \frac{4}{m_\kappa} [\nu_\kappa \sin \pi q_y \sin \pi q_z] = M_{zy} \begin{pmatrix} \vec{q} \\ \kappa\kappa \end{pmatrix} \\
 M_{zx} \begin{pmatrix} \vec{q} \\ \kappa\kappa \end{pmatrix} &= \frac{4}{m_\kappa} [\nu_\kappa \sin \pi q_z \sin \pi q_x] = M_{xz} \begin{pmatrix} \vec{q} \\ \kappa\kappa \end{pmatrix}
 \end{aligned}
 \tag{2.15}$$

$$\begin{aligned}
 M_{\alpha\alpha} \begin{pmatrix} \vec{q} \\ 12 \end{pmatrix} &= -\frac{\alpha}{\sqrt{m_\kappa m_\kappa}} [\exp \frac{\pi i}{2} (q_x + q_y + q_z) + \exp \frac{\pi i}{2} (q_z - q_x - q_y) \\
 &\quad + \exp \frac{\pi i}{2} (q_y - q_x - q_z) + \exp \frac{\pi i}{2} (q_x - q_y - q_z)]
 \end{aligned}
 \tag{2.16}$$

where $\alpha = x, y, z$

$$\begin{aligned}
 M_{xy} \begin{pmatrix} \vec{q} \\ 12 \end{pmatrix} &= -\frac{\beta}{\sqrt{m_k m_l}} \left[\exp \frac{\pi i}{2} (q_x + q_y + q_z) + \exp \frac{\pi i}{2} (q_z - q_x - q_y) \right. \\
 &\quad \left. - \exp \frac{\pi i}{2} (q_y - q_x - q_z) - \exp \frac{\pi i}{2} (q_x - q_y - q_z) \right] = M_{yx} \begin{pmatrix} \vec{q} \\ 12 \end{pmatrix} \\
 M_{yz} \begin{pmatrix} \vec{q} \\ 12 \end{pmatrix} &= -\frac{\beta}{\sqrt{m_k m_l}} \left[\exp \frac{\pi i}{2} (q_x + q_y + q_z) - \exp \frac{\pi i}{2} (q_z - q_x - q_y) \right. \\
 &\quad \left. - \exp \frac{\pi i}{2} (q_y - q_x - q_z) + \exp \frac{\pi i}{2} (q_x - q_y - q_z) \right] = M_{zy} \begin{pmatrix} \vec{q} \\ 12 \end{pmatrix} \\
 M_{zx} \begin{pmatrix} \vec{q} \\ 12 \end{pmatrix} &= -\frac{\beta}{\sqrt{m_k m_l}} \left[\exp \frac{\pi i}{2} (q_x + q_y + q_z) - \exp \frac{\pi i}{2} (q_z - q_x - q_y) \right. \\
 &\quad \left. + \exp \frac{\pi i}{2} (q_y - q_x - q_z) - \exp \frac{\pi i}{2} (q_x - q_y - q_z) \right] = M_{xz} \begin{pmatrix} \vec{q} \\ 12 \end{pmatrix}
 \end{aligned}
 \tag{2.17}$$

$$M_{\alpha\beta} \begin{pmatrix} \vec{q} \\ 21 \end{pmatrix} = M_{\alpha\beta}^* \begin{pmatrix} \vec{q} \\ 12 \end{pmatrix}
 \tag{2.18}$$

where $M_{\alpha\beta}^* \begin{pmatrix} \vec{q} \\ 12 \end{pmatrix}$ is the hermitian conjugate of $M_{\alpha\beta} \begin{pmatrix} \vec{q} \\ 12 \end{pmatrix}$. κ can be either 1 or 2 depending upon the type of the lattice particle.

The equations (2.16 and 2.17) are different from the similar matrix elements of Smith, which are incorrect since a factor $\exp \frac{\pi i}{2} (q_x + q_y + q_z)$ is left out in her paper²⁷.

Thus, if we know the direction and assign particular values to the parameters we can calculate the normal mode of vibrations for that direction in the reciprocal space.

UNIVERSITY OF CALIFORNIA

Next, we try to find a relation between the force constants and elastic constants. According to Born, one can deduce the relation between the coupling parameters and the elastic constants by taking the long wave length limit of the acoustic branch of the lattice vibrations. If we develop the terms of the equation of motion

$$\omega^2 \psi(k) = \sum_{K'} C_{\alpha\beta} \left(\begin{matrix} \vec{q} \\ KK' \end{matrix} \right) \cdot \psi(K') \quad (2.19)$$

where

$$C_{\alpha\beta} \left(\begin{matrix} \vec{q} \\ KK' \end{matrix} \right) = \Phi_{\alpha\beta} e^{-i \left(\vec{q} \cdot \vec{r} \left(\begin{matrix} 1 \\ KK' \end{matrix} \right) \right)} \quad (2.20)$$

as

$$C_{\alpha\beta} \left(\begin{matrix} \vec{q} \\ KK' \end{matrix} \right) = C^{(0)} \left(\begin{matrix} \vec{q} \\ KK' \end{matrix} \right) + C^{(1)} \left(\begin{matrix} \vec{q} \\ KK' \end{matrix} \right) + C^{(2)} \left(\begin{matrix} \vec{q} \\ KK' \end{matrix} \right) + \dots \quad (2.21)$$

The first three terms on the right hand side of eq.

(2.21) have the explicit form

$$\begin{aligned} C^{(0)} \left(\begin{matrix} \vec{q} \\ KK' \end{matrix} \right) &= \sum_1 \Phi \left(\begin{matrix} \vec{q} \\ KK' \end{matrix} \right) \\ C^{(1)} \left(\begin{matrix} \vec{q} \\ KK' \end{matrix} \right) &= -i \sum_1 \Phi \left(\begin{matrix} \vec{q} \\ KK' \end{matrix} \right) \left[\vec{r} \left(\begin{matrix} 1 \\ KK' \end{matrix} \right) \cdot \vec{q} \right] \\ C^{(2)} \left(\begin{matrix} \vec{q} \\ KK' \end{matrix} \right) &= -\frac{1}{2} \sum_1 \Phi \left(\begin{matrix} \vec{q} \\ KK' \end{matrix} \right) \left[\vec{r} \left(\begin{matrix} 1 \\ KK' \end{matrix} \right) \cdot \vec{q} \right]^2 \end{aligned} \quad (2.22)$$

Equating terms containing like powers of \vec{q} on either side of equation (2.19), the equation of motion can be approximated as

$$\sum_{\beta \kappa'} C_{\alpha\beta}^{(0)} \left(\vec{q} \right)_{\kappa\kappa'} \mathcal{V}_{\beta}^{(1)}(\kappa') + \sum_{\beta \kappa'} \sqrt{m_{\kappa'}} C_{\alpha\beta}^{(1)} \left(\vec{q} \right)_{\kappa\kappa'} \mathcal{V}_{\beta} = 0 \quad (2.23)$$

$$\begin{aligned} \left(\sum_{\kappa} m_{\kappa} \right) \omega^2 \mathcal{V}_{\alpha} &= \sum_{\kappa\kappa'} \sum_{\beta} \sqrt{m_{\kappa}} C_{\alpha\beta}^{(1)} \left(\vec{q} \right)_{\kappa\kappa'} \mathcal{V}_{\beta}^{(1)}(\kappa') \\ &+ \sum_{\kappa\kappa'} \sqrt{m_{\kappa} m_{\kappa'}} C_{\alpha\beta}^{(2)} \left(\vec{q} \right)_{\kappa\kappa'} \mathcal{V}_{\beta} \end{aligned} \quad (2.24)$$

Eliminating $\mathcal{V}_{\beta}^{(1)}(\kappa')$ between the equation (2.23)

and (2.24); we can write

$$\rho \omega^2 \mathcal{V}_{\alpha} = \sum \bar{\Phi}'_{\alpha\beta}(q) \mathcal{V}_{\beta} \quad (2.25)$$

where $\rho = \frac{1}{a} \sum_{\kappa} m_{\kappa}$ is the density and $\mathcal{V}_a = \vec{a}_1 \cdot \vec{a}_2 \times \vec{a}_3 = 2a^3$ is the volume of the unit cell (eq. 2.8).

We compare equation (2.25) with the equation for the amplitudes of elastic waves in elasticity theory and find that the $\bar{\Phi}'_{\alpha\beta}(q)$ are related to the elastic constants in the following way:

$$\begin{bmatrix} \Phi'_{11} (q) \\ \Phi'_{22} (q) \\ \Phi'_{33} (q) \\ \Phi'_{44} (q) \\ \Phi'_{55} (q) \\ \Phi'_{66} (q) \end{bmatrix} = \begin{bmatrix} c_{11} & c_{66} & c_{55} & c_{65} & c_{51} & c_{16} \\ c_{66} & c_{22} & c_{44} & c_{24} & c_{46} & c_{62} \\ c_{55} & c_{44} & c_{33} & c_{43} & c_{35} & c_{54} \\ c_{65} & c_{24} & c_{43} & \frac{1}{2} (c_{23} + c_{44}) & \frac{1}{2} (c_{45} + c_{36}) & \frac{1}{2} (c_{64} + c_{25}) \\ c_{51} & c_{46} & c_{35} & \frac{1}{2} (c_{45} + c_{36}) & \frac{1}{2} (c_{31} + c_{55}) & \frac{1}{2} (c_{56} + c_{14}) \\ c_{16} & c_{62} & c_{54} & \frac{1}{2} (c_{64} + c_{25}) & \frac{1}{2} (c_{56} + c_{14}) & \frac{1}{2} (c_{12} + c_{66}) \end{bmatrix} \begin{bmatrix} q_x^2 \\ q_y^2 \\ q_z^2 \\ 2 q_y q_z \\ 2 q_z q_x \\ 2 q_x q_y \end{bmatrix}$$

Proceeding in a way similar to Smith*, we obtain:

$$\begin{bmatrix} \Phi_{11}^i(q) \\ \Phi_{22}^i(q) \\ \Phi_{33}^i(q) \\ \Phi_{44}^i(q) \\ \Phi_{55}^i(q) \\ \Phi_{66}^i(q) \end{bmatrix} = \frac{1}{2a} \begin{bmatrix} A & B & B & 0 & 0 & 0 \\ B & A & B & 0 & 0 & 0 \\ B & B & A & 0 & 0 & 0 \\ 0 & 0 & 0 & C & 0 & 0 \\ 0 & 0 & 0 & 0 & C & 0 \\ 0 & 0 & 0 & 0 & 0 & C \end{bmatrix} \begin{bmatrix} q_x^2 \\ q_y^2 \\ q_z^2 \\ 2 q_y q_z \\ 2 q_z q_x \\ 2 q_x q_y \end{bmatrix} \quad (2.27)$$

where:

$$A = \alpha + 4 \mu_1 + 4 \mu_2$$

$$B = \alpha - \frac{\beta^2}{\alpha} + 2 (\mu_1 + \mu_2 + \lambda_1 + \lambda_2)$$

$$C = \frac{1}{2} \beta \left(2 - \frac{\beta}{\alpha} \right) + 2 (\nu_1 + \nu_2)$$

* It should always be kept in mind that there is only one kind of particle in Smith's treatment whereas the two kind of particles in zinc blende lattice has different masses.

The elastic constants can thus be given as

$$\begin{aligned}c_{11} &= \frac{1}{2a} (\alpha + 4 \mu_1 + 4 \mu_2) \\c_{44} &= \frac{1}{2a} \left\{ \alpha - \frac{\beta^2}{\alpha} + 2 (\lambda_1 + \lambda_2) + 2 (\mu_1 + \mu_2) \right\} \\c_{12} &= \frac{1}{2a} \left\{ 2 \beta - \alpha - 2 (\lambda_1 + \lambda_2) - 2 (\mu_1 + \mu_2) + 4 (\nu_1 + \nu_2) \right\}\end{aligned}\tag{2.28}$$

B) Coulomb Part

We now include the terms which arise from the electrostatic interaction of units within the crystal. Since every atom situated at the lattice points can be considered as an ion and in two neighbouring lattice points, the ions are of different polarity we can consider them as dipoles. Thus the crystal field can be assumed to be a field of dipoles. In the similar manner if we consider Cochran shell model we can see that the relative displacement of a core and a shell produces a dipole which in turn exerts some influence on the other units of the crystal. The forces exerted due to these dipoles and their effective contribution to the coupling coefficients were shown by Kellermann in 1942.

He has defined the Coulomb coefficients in his work for NaCl lattice. Cochran has applied this definition to diamond and we can extend it to zinc blende lattice.

From Cochran's paper it follows that

$$c_{C_{\alpha\beta}}(\vec{q}) = -Z^2 e^2 \lim \left[\sum_{\vec{r}}' \frac{\partial^2}{\partial \alpha \partial \beta} \frac{\exp(i \vec{q} \cdot \vec{r})}{|\vec{r} - \vec{r}_\alpha|} \right] \quad (2.29)$$

$$c_{C_{\alpha\beta}}(\vec{q}) = -Z^2 e^2 \left\{ \exp(i \vec{q} \cdot \vec{r}_{1,2}) \lim_{\vec{r} \rightarrow -\vec{r}_{1,2}} \left[\sum_{\vec{r}}' \frac{\partial^2 \exp(i \vec{q} \cdot \vec{r}_l)}{\partial \alpha \partial \beta} \frac{1}{|\vec{r} - \vec{r}_l|} \right] \right\} \quad (2.30)$$

We have used a slightly different notation with the abbreviation

$$\vec{r}_i = \vec{r}_i(l) \quad (2.31)$$

Modifying for the zinc blende lattice, we can write

$$\begin{aligned} \vec{r}_I(l) &= a (l_2 + l_3, l_3 + l_1, l_1 + l_2) \\ &= a (l_x, l_y, l_z) \end{aligned} \quad (2.32)$$

where $\sum l_x = 2N$

$$\begin{aligned} \text{and } \vec{r}_{II}(l) &= a (l_2 + l_3 + \frac{1}{2}, l_3 + l_1 + \frac{1}{2}, l_1 + l_2 + \frac{1}{2}) \\ &= a (m_x, m_y, m_z) \end{aligned} \quad (2.32b)$$

where $\sum m_x = 2N + \frac{3}{2}$

The reciprocal vectors are given by

$$\begin{aligned} \mathbf{b}_1 &= \frac{1}{2a} (-1, 1, 1) \\ \mathbf{b}_2 &= \frac{1}{2a} (1, -1, 1) \\ \mathbf{b}_3 &= \frac{1}{2a} (1, 1, -1) \end{aligned} \quad (2.33)$$

thus a vector in reciprocal space is:

$$\begin{aligned} \mathbf{b}_h &= \frac{1}{2a} (h_2+h_3-h_1, h_3+h_1-h_2, h_1+h_2-h_3) \\ &= \frac{1}{2a} (h_x, h_y, h_z) \end{aligned} \quad (2.34)$$

where h_x, h_y, h_z are either all odd or all even. Since

$$\begin{aligned} &= q_1 \mathbf{b}_1 + q_2 \mathbf{b}_2 + q_3 \mathbf{b}_3 \\ &= \frac{1}{2a} (q_2+q_3-q_1, q_3+q_1-q_2, q_1+q_2-q_3) \\ &= \frac{1}{2a} (q_x, q_y, q_z) \end{aligned} \quad (2.35)$$

we now give Kellermann's formulae for Coulomb coefficients

(for zinc blende lattice modifications)

For $\vec{q} = 0$

$$\frac{a}{Z^2 e^2} c_{\alpha\beta} \left(\begin{array}{c} \vec{q} \\ \kappa\kappa' \end{array} \right) = \frac{4\pi}{3} \delta_{\alpha\beta} \quad (2.36)$$

For other directions $\vec{q} \neq 0$

$$\frac{v_a}{z^2 e^2} c_{\alpha\beta} \left(\begin{array}{c} \vec{q} \\ \kappa\kappa \end{array} \right) = -G_{\alpha\beta}(\kappa\kappa) + H_{\alpha\beta}(\rho) + \frac{8}{3\sqrt{\pi}} \epsilon^3 \delta_{\alpha\beta}$$

$$\frac{v_a}{z^2 e^2} c_{\alpha\beta} \left(\begin{array}{c} \vec{q} \\ 12 \end{array} \right) = G_{\alpha\beta}(12) - H_{\alpha\beta}(n)$$

where

$$G_{\alpha\beta}(\kappa\kappa) = 4 \pi \sum_h \frac{(h_\alpha + q_\alpha)(h_\beta + q_\beta)}{(\vec{h} + \vec{q})^2} \exp \left[-\frac{\pi^2}{4\epsilon^2} (\vec{h} + \vec{q})^2 \right]$$

$$G_{\alpha\beta}(12) = 4 \pi \sum_h \frac{(h_\alpha + q_\alpha)(h_\beta + q_\beta)}{(\vec{h} + \vec{q})^2} \exp \left[-\frac{\pi^2}{4\epsilon^2} (\vec{h} + \vec{q})^2 \right]$$

$$\exp(i\pi(h_x + h_y + h_z))$$

(2.37)

$$H_{\alpha\beta}(\rho) = 2 \sum_{\vec{l}} [-f(\vec{l}) \delta_{\alpha\beta} + g(l) \frac{l_\alpha l_\beta}{|\vec{l}|^2} \exp(i\pi \vec{q} \cdot \vec{l})]$$

(($\vec{l} = 0$) excluded)

(2.38)

$$f(\vec{l}) = \frac{2}{\sqrt{\pi}} \frac{\exp(-\epsilon^2 l^2)}{l^2} + \frac{\psi(\epsilon l)}{l^3}$$

$$g(l) = \frac{4}{\sqrt{\pi}} \epsilon^3 \exp(-\epsilon^2 l^2) + \frac{6}{\sqrt{\pi}} \epsilon \frac{\exp(-\epsilon^2 l^2)}{l^2} + \frac{3 \psi(\epsilon l)}{l^3}$$

(2.39)

$$\psi(\epsilon l) = 1 - \frac{2}{\sqrt{\pi}} \int_0^\epsilon \exp(-\xi^2) d\xi$$

(2.40)

with $l = |\vec{l}| = \sqrt{l_x^2 + l_y^2 + l_z^2}$

(2.41)

These equations only hold for $\vec{q} \neq (0, 0, 0)$ should be remembered for numerical calculations.

4. Dynamical Matrices and Elastic Constants For SNI Model

The dynamical matrix can be written as a combination of the mechanical and Coulomb part.

$$C_{\alpha\beta} \left(\begin{smallmatrix} q \\ \kappa\kappa' \end{smallmatrix} \right) = m_{C_{\alpha\beta}} \left(\begin{smallmatrix} q \\ \kappa\kappa' \end{smallmatrix} \right) - c_{C_{\alpha\beta}} \left(\begin{smallmatrix} q \\ \kappa\kappa' \end{smallmatrix} \right)$$

where we slightly change the notation by saying $m_{C_{\alpha\beta}} \left(\begin{smallmatrix} q \\ \kappa\kappa' \end{smallmatrix} \right)$ as the contribution from the mechanical part and $c_{C_{\alpha\beta}} \left(\begin{smallmatrix} q \\ \kappa\kappa' \end{smallmatrix} \right)$ as the dynamical matrix element.

Thus we can write the dynamical matrix as

$$\begin{bmatrix}
 \frac{1}{m_1} C_{xx} & (11) & \frac{1}{m_1} C_{xy} & (11) & \frac{1}{m_1} C_{xz} & (11) & \sqrt{\frac{1}{m_1 m_2}} C_{xx} & (12) & \sqrt{\frac{1}{m_1 m_2}} C_{xy} & (12) & \sqrt{\frac{1}{m_1 m_2}} C_{xz} & (12) \\
 \frac{1}{m_1} C_{yx} & (11) & \frac{1}{m_1} C_{yy} & (11) & \frac{1}{m_1} C_{yz} & (11) & \sqrt{\frac{1}{m_1 m_2}} C_{yx} & (12) & \sqrt{\frac{1}{m_1 m_2}} C_{yy} & (12) & \sqrt{\frac{1}{m_1 m_2}} C_{yz} & (12) \\
 \frac{1}{m_1} C_{zx} & (11) & \frac{1}{m_1} C_{zy} & (11) & \frac{1}{m_1} C_{zz} & (11) & \sqrt{\frac{1}{m_1 m_2}} C_{zx} & (12) & \sqrt{\frac{1}{m_1 m_2}} C_{zy} & (12) & \sqrt{\frac{1}{m_1 m_2}} C_{zz} & (12) \\
 \sqrt{\frac{1}{m_1 m_2}} C_{xx}^* & (12) & \sqrt{\frac{1}{m_1 m_2}} C_{xy}^* & (12) & \sqrt{\frac{1}{m_1 m_2}} C_{xz}^* & (12) & \frac{1}{m_2} C_{xx} & (22) & \frac{1}{m_2} C_{xy} & (22) & \frac{1}{m_2} C_{xz} & (22) \\
 \sqrt{\frac{1}{m_1 m_2}} C_{yx}^* & (12) & \sqrt{\frac{1}{m_1 m_2}} C_{yy}^* & (12) & \sqrt{\frac{1}{m_1 m_2}} C_{yz}^* & (12) & \frac{1}{m_2} C_{yx} & (22) & \frac{1}{m_2} C_{yy} & (22) & \frac{1}{m_2} C_{yz} & (22) \\
 \sqrt{\frac{1}{m_1 m_2}} C_{zx}^* & (12) & \sqrt{\frac{1}{m_1 m_2}} C_{zy}^* & (12) & \sqrt{\frac{1}{m_1 m_2}} C_{zz}^* & (12) & \frac{1}{m_2} C_{zx} & (22) & \frac{1}{m_2} C_{zy} & (22) & \frac{1}{m_2} C_{zz} & (22)
 \end{bmatrix}$$

This matrix is hermitian and hence it can be easily diagonalized to obtain the characteristic frequencies.

The expressions for the elastic constants (Blackman 1958)³³ can now be given as:

$$c_{11} = 0.1255 \frac{z^2 e^2}{2a^4} + \frac{(\alpha + 4 \mu_1 + 4 \mu_2)}{2a}$$

$$c_{12} = -1.324 \frac{z^2 e^2}{2a^4} + \frac{1}{2a} \{2 \beta - \alpha - 2 (\lambda_1 + \lambda_2) - 2 (\mu_1 + \mu_2) + 4 (v_1 + v_2)\}$$

$$c_{44} = -0.063 \frac{z^2 e^2}{2a^4} + \frac{1}{2a} \{\alpha + 2 (\lambda_1 + \lambda_2) + 2 (\mu_1 + \mu_2)\} - A^2/B$$

where $A = 2.519 \frac{z^2 e^2}{2a^5} - \frac{\beta}{a^2}$

$$B = (4\alpha - 4\pi \frac{z^2 e^2}{6a^3})/2a^3$$

CHAPTER III

KAPLAN AND SULLIVAN'S MODEL

This model is basically a shell model and hence it can be summarized by saying that the interactions are due to core-core (CC), shell-shell (SS) and each of the two types of core and shell interactions. There are separate second neighbour matrices for the two types of atoms in the unit cell, and for each of these there are core-core, shell-shell, core-shell and shell-core interactions. The shell charges are Y_1 and Y_2 and the core charges are X_1 and X_2 . The total ionic charges are

$$Z_1 = Y_1 + X_1, \quad Z_2 = X_2 + Y_2$$

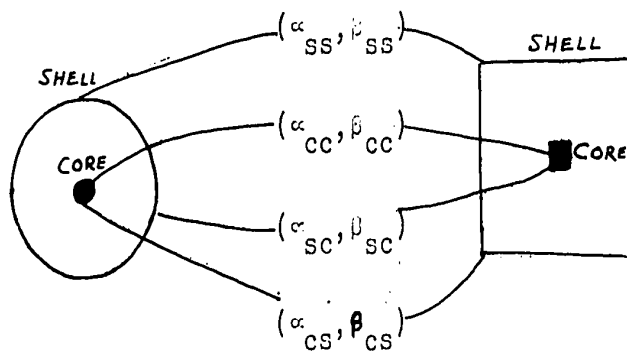


Figure 3.1: The most general nearest neighbour shell model for zinc blende structure vibration showing the force constants and charges.

Charge neutrality requires $Z_1 + Z_2 = 0$. The constant k_1 and k_2 represent isotropic coupling of each core to its own shell. With the parameters of KS model specified we may follow the procedure indicated in the previous shell model^{15, 16, 17} calculations in order to find dispersion curves for different directions in the reciprocal space and expressions for various parameters of interest. The shells and cores are treated as separate degrees of freedom, but since the shells are mass less the equations of motion for the shells do not add additional branches to the vibration spectrum. These equations establish a relation between core and shell displacements and thus serve to eliminate the shell displacements from the core equations of motion, while simultaneously introducing the shell polarization effects into the core motions. We will write down a few important formulae here without going to more details:

The dispersion curves are obtained by solving

$$|M_{\alpha\beta}(\vec{q}, \kappa\kappa') - \omega^2(\vec{q}, j) \delta_{\kappa\kappa'} \delta_{\alpha\beta}| = 0 \quad (3.1)$$

UNIVERSITY OF OTTAWA

where \vec{q} is the wave vector, j is the branch of the vibration spectra, α and β are cartesian indices, and κ and κ' are indices corresponding to the different cores in the unit cell. The relative amplitudes of the various cores in the normal mode \vec{q} , j are obtained from the equations.

$$\omega^2(\vec{q}, j) \omega_\alpha(\kappa) = \sum_{\kappa'\beta} M_{\alpha\beta}(\vec{q}, \kappa\kappa') \omega_\beta(\kappa') \quad (3.2)$$

The time dependent core amplitudes in a normal mode are

$$u_\alpha^c(\kappa, l) = (m_\kappa)^{-1/2} \exp \{ 2\pi i \vec{q} \cdot (\vec{x}(l) + \vec{x}(\kappa) - i\omega t) \} \omega_\alpha(\kappa) \quad (3.3)$$

and the shell amplitudes are

$$u_\alpha^s(\kappa, l) = -\exp \{ 2 \pi i \vec{q} \cdot [\vec{x}(l) + \vec{x}(\kappa)] - i\omega t \} Y \quad (3.4)$$

where

$$Y = \sum_{\nu, \beta, \kappa_1, \kappa'} D_{\alpha\nu}^{ss}(\kappa\kappa_1) C_{\nu\beta}^{sc}(\kappa\kappa') \omega_{\alpha\beta}(\kappa') / (m_{\kappa'})^{1/2} \quad (3.5)$$

where $\vec{x}(l) + \vec{x}(\kappa)$ is the undisplaced position of a core or shell at the κ th site in the l th unit cell. [The matrix elements $M_{\alpha\beta}(\vec{q}, \kappa\kappa')$ of KS model and $C_{\alpha\beta}(\frac{q}{\kappa\kappa'})$ of SNI model are of the similar form and also the secular equation, but since we are considering the two different models the two secular

equations are taken separately.] The matrix elements $M_{\alpha\beta}$

$(\vec{q}, \kappa\kappa')$ are given by

$$M_{\alpha\beta}(\vec{q}, \kappa\kappa') = [M_{\kappa\kappa'}]^{-1/2} \{ C_{\alpha\beta}^{CC}(\kappa\kappa') - \sum_{\gamma, \delta, \kappa_1, \kappa_2} C_{\alpha\gamma}^{CS}(\kappa\kappa_1) D_{\gamma\delta}^{SS}(\kappa_1\kappa_2) C_{\delta\beta}^{SC}(\kappa_2\kappa') \} \quad (3.6)$$

where

$$D^{SS} = (C^{SS})^{-1}$$

and the C matrices are given by

$$C_{\alpha\beta}^{CC}(\kappa\kappa') = \sum_{l'} \exp \{ 2\pi i \vec{q} \cdot (\vec{x}(l') + \vec{x}(\kappa') - \vec{x}(l) - \vec{x}(\kappa)) \} \cdot \Phi_{\alpha\beta}^{CC}(l-l', \kappa\kappa') \quad (3.7)$$

with similar expressions for $C_{\alpha\beta}^{CS}(\kappa\kappa')$, $C_{\alpha\beta}^{SC}(\kappa\kappa')$ and $C_{\alpha\beta}^{SS}(\kappa\kappa')$.

Here the Φ 's are the force constants connecting the indicated degrees of freedom. Note that the first shell or core superscript belongs to the particle κ and the second with particle κ' . It may be pointed out that these dynamical matrix elements are the same as in the SNI model except the force constants will be different for core-core, core-shell, shell-core and shell-shell interactions. Thus the elements should also consist of Coulomb interactions. Keeping this in mind one should try

to write down the elements of the dynamical matrix. The parameters for this can be evaluated. Once, the parameters are known if we follow Kaplan's notations we can expand the constituents of the dynamical elements in the following way:

The matrix $C_{\alpha\beta}^{CC}(\kappa\kappa')$ can be written in a similar manner as in SNI model (eq. 2.14 to 2.17) with the same kind of parameters.

For $C_{\alpha\beta}^{SS}(\kappa\kappa')$ we must remember that it can be expanded as

$$C_{\alpha\beta}^{SS}(\kappa\kappa') = \begin{pmatrix} C_{\alpha\beta}^{SS}(\kappa_1\kappa_1) & C_{\alpha\beta}^{SS}(\kappa_1\kappa_2) \\ C_{\alpha\beta}^{SS}(\kappa_2\kappa_1) & C_{\alpha\beta}^{SS}(\kappa_2\kappa_2) \end{pmatrix} \quad (3.8)$$

i.e. in a combination of four 3×3 matrices. For the first matrix $C_{\alpha\beta}^{SS}(\kappa_1\kappa_1)$ the force constant α_1 (as in Kaplan), α_2 in $C_{\alpha\beta}^{SS}(\kappa_2\kappa_2)$ and $G/4$ and $H/4$ in both $C_{\alpha\beta}^{SS}(\kappa_1\kappa_2)$ and $C_{\alpha\beta}^{SS}(\kappa_2\kappa_1)$ should be used. It is useful to remember that the matrix is hermitian.

Similarly, for the matrices due to the shell-core and core-shell interactions, we have $C_{\alpha\beta}^{SC}(\kappa\kappa')$ and $C_{\alpha\beta}^{CS}(\kappa\kappa')$

UNIVERSITY OF OTTAWA

which can be given as

$$C_{\alpha\beta}^{SC}(\kappa\kappa') = \begin{pmatrix} C_{\alpha\beta}^{SC}(\kappa_1\kappa_1) & C_{\alpha\beta}^{SC}(\kappa_1\kappa_2) \\ C_{\alpha\beta}^{SC}(\kappa_2\kappa_1) & C_{\alpha\beta}^{SC}(\kappa_2\kappa_2) \end{pmatrix} \quad (3.9)$$

and

$$C_{\alpha\beta}^{CS}(\kappa\kappa') = \begin{pmatrix} C_{\alpha\beta}^{CS}(\kappa_1\kappa_1) & C_{\alpha\beta}^{CS}(\kappa_1\kappa_2) \\ C_{\alpha\beta}^{CS}(\kappa_2\kappa_1) & C_{\alpha\beta}^{CS}(\kappa_2\kappa_2) \end{pmatrix} \quad (3.10)$$

i.e. combinations of 3 x 3 matrices. Obviously, $C_{\alpha\beta}^{SC}(\kappa_i\kappa_i)$ and $C_{\alpha\beta}^{CS}(\kappa_i\kappa_i)$ are the same whereas $C_{\alpha\beta}^{SC}(\kappa_1\kappa_2)$ and $C_{\alpha\beta}^{SC}(\kappa_2\kappa_1)$ are complex conjugates of $C_{\alpha\beta}^{CS}(\kappa_2\kappa_1)$ and $C_{\alpha\beta}^{CS}(\kappa_1\kappa_2)$ respectively.

These two matrices are not hermitian but it can be showed that the product of the three matrices

$$C_{\alpha\beta}^{CS}(\kappa\kappa'), D_{\alpha\beta}^{SS}(\kappa\kappa') \text{ and } C_{\alpha\beta}^{SC}(\kappa\kappa')$$

is hermitian (see Appendix I) where $D_{\alpha\beta}^{SS}$ is the inverse of $C_{\alpha\beta}^{SS}(\kappa\kappa')$ and hence will remain hermitian.

The matrix $M_{\alpha\beta}(\vec{q}, \kappa\kappa')$ is difference of two hermitian matrices, hence will remain hermitian and can easily be diagonalized.

CHAPTER IV

THE SECULAR EQUATIONS FOR THE SPECIAL DIRECTIONS

We would like to show the method of solving the secular equations in the special directions for both the models.

In SNI model, it has been seen that by taking into account the Coulomb interaction, an effective charge Ze is postulated on the ions. The coupling coefficients now consist of two parts

$$C_{\alpha\beta} \left(\begin{matrix} q \\ KK' \end{matrix} \right) = m C_{\alpha\beta} \left(\begin{matrix} q \\ KK' \end{matrix} \right) - c C_{\alpha\beta} \left(\begin{matrix} q \\ KK \end{matrix} \right) \quad (2.42)$$

When we are considering KS model, it can be shown very easily that though the individual dynamical matrix elements will be different, the general pattern, i.e. the symmetry, zeros etc. will have the same form as SNI model. This is due to the fact that the individual matrix elements of core-core, core-shell and shell-shell follow the same pattern as that of SNI model and the way the matrix equation (eq. 3.6) is set up the general pattern

will be retained. The following treatment thus can be applied for both the models.

The dynamical matrix can always be written as:

$$M_{\alpha\beta} \begin{pmatrix} q \\ KK \end{pmatrix} = \begin{pmatrix} M_{\alpha\beta} \begin{pmatrix} q \\ 11 \end{pmatrix} & M_{\alpha\beta} \begin{pmatrix} q \\ 12 \end{pmatrix} \\ M_{\alpha\beta} \begin{pmatrix} q \\ 21 \end{pmatrix} & M_{\alpha\beta} \begin{pmatrix} q \\ 22 \end{pmatrix} \end{pmatrix} \quad (4.1)$$

where $M_{\alpha\beta} \begin{pmatrix} q \\ 11 \end{pmatrix}$, etc. are each 3 x 3 matrices.

We consider only two special directions in the Brillouin zone, namely [100] and [111] directions.

If we also take into account the tables of Kellermann's coefficients in Cochran's paper, we can easily find the dynamical matrix elements and the secular equation thus can be written for the special directions:

[100] direction:

The secular equation in [100] direction can be shown to be as follows:

UNIVERSITY OF OTTAWA

$$\begin{array}{cccccc|c}
 S'_1 & 0 & 0 & V & 0 & 0 & \\
 0 & U'_1 & 0 & 0 & W & X & \\
 0 & 0 & U'_1 & 0 & X & W & \\
 V^* & 0 & 0 & S'_2 & 0 & 0 & = 0 \quad (4.2) \\
 0 & W^* & X^* & 0 & U'_2 & 0 & \\
 0 & X^* & W^* & 0 & 0 & U'_2 &
 \end{array}$$

where

$$S'_1 = S_1 - w^2 \text{ and } S'_2 = S_2 - w^2 \quad (4.3)$$

and

$$\begin{aligned}
 S_1 &= M_{xx} \binom{q}{11}, & S_2 &= M_{xx} \binom{q}{22} \\
 U_1 &= M_{yy} \binom{q}{11} = M_{zz} \binom{q}{11} \\
 U_2 &= M_{yy} \binom{q}{22} = M_{zz} \binom{q}{22} \\
 V &= M_{xx} \binom{q}{12} \\
 W &= M_{yy} \binom{q}{12} = M_{zz} \binom{q}{12} \\
 X &= M_{yz} \binom{q}{12} = M_{zy} \binom{q}{12}
 \end{aligned} \quad (4.4)$$

By interchanging the rows and the columns and after other manipulations

$$\begin{vmatrix} S'_1 & V \\ V^* & S'_2 \end{vmatrix} \begin{vmatrix} U'_1 & W-X \\ W^*-X^* & U'_2 \end{vmatrix} \begin{vmatrix} U'_1 & W+X \\ W^*+X^* & U'_2 \end{vmatrix} = 0 \quad (4.5)$$

and hence

$$\begin{aligned}
\omega_1^2 &= \frac{U_1 + U_2}{2} \pm \sqrt{\left(\frac{U_1 - U_2}{2}\right)^2 + |W - X|^2} \\
\omega_2^2 &= \frac{U_1 + U_2}{2} \pm \sqrt{\left(\frac{U_1 - U_2}{2}\right)^2 + |W + X|^2} \\
\omega_3^2 &= \frac{S_1 + S_2}{2} \pm \sqrt{\left(\frac{S_1 - S_2}{2}\right)^2 + |V|^2}
\end{aligned}
\tag{4.6}$$

Since $|W + X|^2 = |W - X|^2$, we will have

$$\begin{aligned}
\omega_1^2 &= \omega_2^2 = \omega_L^2 \\
\text{and } \omega_3^2 &= \omega_T^2
\end{aligned}
\tag{4.7}$$

Out of these four different roots of ω^2 ; ω_L^2 are the longitudinal vibrations and ω_T^2 are the transverse vibrations.

Each kind of vibration will have the optical and the acoustic branches. This will depend upon the choice of positive or negative sign in the right hand side of equation (4.6) - the positive sign gives the optical branch and the negative sign gives the acoustic.

[111] direction:

The secular equation for [111] direction has the expression:

UNIVERSITY OF OTTAWA

$$\begin{array}{cccccc|c}
 U'_1 & V_1 & V_1 & W & X & X & \\
 V_1 & U'_1 & V_1 & X & W & X & \\
 V_1 & V_1 & U'_1 & X & X & W & \\
 W^* & X^* & X^* & U'_2 & V_2 & V_2 & = 0 \quad (4.8) \\
 X^* & W^* & X^* & V_2 & U'_2 & V_2 & \\
 X^* & X^* & W^* & V_2 & V_2 & U'_2 &
 \end{array}$$

where

$$\begin{aligned}
 U'_1 &= U_1 - \omega^2, \quad U'_2 = U_2 - \omega^2 \\
 U_1 &= M_{\alpha\alpha} \begin{pmatrix} q \\ 11 \end{pmatrix}, \quad U_2 = M_{\alpha\alpha} \begin{pmatrix} q \\ 22 \end{pmatrix} \\
 V_1 &= M_{\alpha\beta} \begin{pmatrix} q \\ 11 \end{pmatrix}, \quad V_2 = M_{\alpha\beta} \begin{pmatrix} q \\ 22 \end{pmatrix} \\
 W &= M_{\alpha\alpha} \begin{pmatrix} q \\ 12 \end{pmatrix}, \quad X = M_{\alpha\beta} \begin{pmatrix} q \\ 12 \end{pmatrix} \\
 \alpha, \beta &= x, y, z \\
 \text{and } \alpha &\neq \beta
 \end{aligned}$$

after the usual manipulations:

$$\begin{vmatrix} U'_1 - V_1 & W - X \\ W^* - X^* & U'_2 - V_2 \end{vmatrix}^2 - \begin{vmatrix} U'_1 + 2V_1 & W + 2X \\ W + 2X & U'_2 + 2V_2 \end{vmatrix} = 0 \quad (4.10)$$

and similar to eq. (4.6)

$$\omega_T^2 = \frac{U_1 - V_1}{2} + \frac{U_2 - V_2}{2} \pm \sqrt{\left(\frac{U_1 - V_1}{2} - \frac{U_2 - V_2}{2}\right)^2 + |W - X|^2} \quad (4.11)$$

$$\omega_L^2 = \frac{U_1 + 2V_2}{2} + \frac{U_2 + 2V_1}{2} \pm \sqrt{\left(\frac{U_1 + 2V_1}{2} - \frac{U_2 + 2V_2}{2}\right)^2 + |W + 2X|^2}$$

These two kinds of vibrations again, will have the optical and the acoustic branches depending upon the choice of sign in the right hand side of eq. (4.11).

Next, we must show what happens in SNI model at the [000] point (Γ) in the Brillouin zone, the frequency at this point is the Raman frequency of the lattice:

$$\omega_T^2 = (4 \alpha - \frac{4\pi}{6} x) \left(\frac{1}{m_1} + \frac{1}{m_2}\right)$$

and

$$\omega_L^2 = (4 \alpha + \frac{8\pi}{6} x) \left(\frac{1}{m_1} + \frac{1}{m_2}\right)$$

where $x = \frac{Z^2 e^2}{a^3}$

Thus we have all the information for calculating the parameters from the special direction values.

The expressions given in Kaplan and Sullivan's paper (eq. 9) can easily be shown to follow from the determinant (eqs. 4.2 and 4.8)*.

* It may be mentioned here that there appears to be a misprint in the expression (9c,d) of Kaplan and Sullivan; the correct expression is

$$\omega(T_1, T_2)^2 = \frac{SM_1 + SM_2 \pm [(SM_1 - QM_2)^2 + 4R^2 M_1 M_2]^{1/2}}{2 M_1 M_2}$$

CHAPTER V

DETERMINATION OF PARAMETERS

In order to determine the parameters for SNI model, we first of all take the Raman frequencies and estimate the values of α and x

$$\begin{aligned}\omega_T^2 &= (4\alpha - \frac{4\pi}{6} x) (m^*)^{-1} \\ \omega_L^2 &= (4\alpha + \frac{8\pi}{6} x) (m^*)^{-1}\end{aligned}\tag{4.12}$$

where $m^* = \frac{1}{\frac{1}{m_1} + \frac{1}{m_2}}$

Thus

$$\begin{aligned}\alpha &= \frac{m^*}{12} (\omega_L^2 + 2 \omega_T^2) \\ x &= \frac{m^*}{2\pi} (\omega_L^2 - \omega_T^2)\end{aligned}\tag{5.1}$$

Next, we use the zone boundary frequencies in the direction [100] to calculate the other parameters

$$\omega_L^2 = \frac{S_1}{2} + \frac{S_2}{2} \pm \sqrt{\left(\frac{S_1 - S_2}{2}\right)^2 + |V|^2}\tag{5.2}$$

but since $V = 0$ in SNI model for this special direction,

$$\begin{aligned}\omega_{LO}^2 &= S_1 \\ \omega_{LA}^2 &= S_2\end{aligned}\tag{5.3}$$

where $m_1 < m_2$, as longitudinal optic frequency should be greater than the longitudinal acoustic frequency.

Considering Kellermann coefficients, we can write

$$\begin{aligned} S_1 &= \frac{4}{m_1} (\alpha + 4 \mu_1 + 0.54125 x) \\ S_2 &= \frac{4}{m_2} (\alpha + 4 \mu_2 + 0.54125 x) \end{aligned} \tag{5.4}$$

and thus

$$\begin{aligned} \mu_1 &= \frac{1}{4} \left(\frac{m_1 \omega_{LO}^2}{4} - \alpha - 0.54125 x \right) \\ \mu_2 &= \frac{1}{4} \left(\frac{m_2 \omega_{LA}^2}{4} - \alpha - 0.54125 x \right) \end{aligned} \tag{5.5}$$

The choice of these frequencies to determine the parameters is two fold. Firstly, their values are known fairly accurately from the available experimental results on III-V compounds and secondly, their simple relationship with the parameters. We have deviated ourselves from the usual procedure of finding the parameters from the elastic constants, instead, the parameters are obtained from the zone boundary frequencies and the elastic constants are the restraints on their values.

We have found the approximate values of β , λ_1 and λ_2 from the three elastic constants i.e. from their relationship with the parameters. Once the approximate value is known, they are substituted in the equations for the transverse optical and acoustic branches of the frequencies in [100] direction. We readjust their values slightly so that the frequencies are accurately given by the parameters. Next, these parameters were substituted in the equations for determining the frequencies in [100] direction.

In the KS model with $Z = 0$, Kaplan found the values of his parameters from the elastic constants, piezoelectric constants and total and electronic polarizabilities as is given in his paper. They are as follows:

$$K_1 = (\kappa_1 + 4\alpha_{S_2 C_1} + 4\alpha_{S_1 S_2} + 8\mu_{S_1 C_1} + 4\lambda_{S_1 C_1}) / Y_1^2$$

$$K_2 = (\kappa_2 + 4\alpha_{S_1 C_2} + 4\alpha_{S_1 S_2} + 8\mu_{S_2 C_2} + 4\lambda_{S_2 C_2}) / Y_2^2$$

$$G = 4 (\alpha_{SS} + \alpha_{S_1 C_2} + \alpha_{S_2 C_1} + \alpha_{CC})$$

$$H = 4 (\beta_{SS} + \beta_{S_1 C_2} + \beta_{S_2 C_1} + \beta_{CC})$$

$$S_1 = 4 (\alpha_{S_1 C_2} + \alpha_{SS}) / Y_1$$

$$S_2 = 4 (\alpha_{S_2 C_1} + \alpha_{SS}) / Y_2$$

$$h_1 = 4 (\beta_{S_1 C_2} + \beta_{SS}) / Y_1$$

$$h_2 = 4 (\beta_{S_2 C_1} + \beta_{SS}) / Y_2$$

$$G = 4 \alpha_{SS} / (Y_1 Y_2)$$

$$H = 4 \beta_{SS} / (Y_1 Y_2)$$

For $i = 1, 2$

$$K_i = 4 (\mu_{S_i S_i} + 2 \mu_{S_i C_i} + \mu_{C_i C_i})$$

$$L_i = 4 (\lambda_{S_i S_i} + 2 \lambda_{S_i C_i} + \lambda_{C_i C_i})$$

$$N_i = 4 (v_{S_i S_i} + 2 v_{S_i C_i} + v_{C_i C_i})$$

$$k_i = 4 (\mu_{S_i C_i} + \mu_{S_i S_i}) / Y_i$$

$$l_i = 4 (\lambda_{S_i C_i} + \lambda_{S_i S_i}) / Y_i$$

$$n_i = 4 (v_{S_i} C_i + v_{S_i} S_i) / Y_i$$

$$K_i = 4 \mu_{S_i} S_i / Y_i^2$$

$$L_i = 4 \lambda_{S_i} S_i / Y_i^2$$

$$N_i = 4 v_{S_i} S_i / Y_i^2$$

These parameters can be found from the following

equations:

$$2aC_{11} = \frac{1}{4} G + 0.25 Z_1^2 / v + K_1 + K_2$$

$$2aC_{12} = \frac{1}{2} H - \frac{1}{4} G - 2.64 Z_1^2 / v + N_1 + N_2 - \frac{1}{2} (L_1 + L_2 + K_1 + K_2)$$

$$2aC_{44} = \frac{1}{4} G + \frac{1}{2} (L_1 + L_2 + K_1 + K_2) - 0.12 Z_1^2 / v + 10.04 Z_1^2 / a \\ + [1 - (\frac{4\pi}{3v}) \alpha_t]^{-1} [25.2 (\frac{Z_1}{v})^2 \alpha_t - \frac{G}{B}],$$

where

$$B = G (\alpha_1 \alpha_2 - G^2) + \epsilon_1 (\epsilon_2 G - \alpha_2 \epsilon_1) + \epsilon_2 (\epsilon_1 G - \alpha_1 \epsilon_2),$$

and

$$4C = H^2 (\alpha_1 \alpha_2 - G^2) + 2H [h_2 (G \epsilon_1 - \alpha_1 \epsilon_2) + h_1 (G \epsilon_2 - \alpha_2 \epsilon_1)] \\ + 2 h_1 h_2 (\epsilon_1 \epsilon_2 - G G) + h_2^2 (G \alpha_1 - \epsilon_1^2) + h_1^2 (\alpha_2 G - \epsilon_2^2) \\ - (4\pi/3v) [G(h_1 + h_2)^2 + \alpha_2 (H - h_1 Z_1)^2 + \alpha_1 (H + h_2 Z_1)^2 \\ + 2 G (H - h_1 Z_1) (H + h_2 Z_1) + Z_1 (h_1 + h_2) (h_1 \epsilon_2 - h_2 \epsilon_1) - 2(\epsilon_1 + \epsilon_2) (h_1 + h_2) H]$$

$$e_{14} = (2a/v) [1 - (4\pi/3v)\alpha_t]^{-1} [E/4B - 2.51 \alpha_t Z_1/v]$$

where

$$E = Z_1 [H(\alpha_1 \alpha_2 - G^2) + h_1 (\epsilon_2 - \alpha_2 \epsilon_1) + h_2 (G \epsilon_1 - \alpha_1 \epsilon_2)] + (\alpha_2 + G)(-h_1 \epsilon_1 + h_2 G) \\ + (\alpha_1 + G)(-h_2 G + h_1 \epsilon_2) + (\epsilon_1 + \epsilon_2)(-h_1 \epsilon_2 + h_2 \epsilon_1)$$

$$\alpha_e = (\alpha_1 + \alpha_2 + 2) / (\alpha_1 \alpha_2 - G^2)$$

$$\alpha_t = (1/B) [Z_1^2 (\alpha_1 \alpha_2 - G^2) + 2 Z_1 (\epsilon_2 (\alpha_1 + G) - \epsilon_1 (\alpha_2 + G)) + G (\alpha_1 + \alpha_2 + 2G) \\ - (\epsilon_1 + \epsilon_2)^2]$$

Thus, all the parameters can be estimated numerically for different substances and they can be used to calculate the dispersion curves, frequency spectra and specific heat of those substances.

CHAPTER VI

NUMERICAL RESULTS AND CALCULATIONS

Before stating the values of the parameters we have found, we must provide the experimental results which have been obtained in the past years for the III-V compounds. Table I gives the lattice constants, elastic constants and Born's ratio of these compounds and the source from which the results are taken. Table II gives the zone boundary frequencies.

With the help of the experimental results of Table I and Table II, we have calculated the parameters of SNI model given in Table III.

We have not calculated the parameters of Kaplan Sullivan's model but quoted the parameter for which $Z = 0$ from his paper. These are given in Table IV.

Table I
Elastic Constant Data

| Compounds | Lattice Constants | Elastic Constants | | | |
|----------------------|---------------------|--|----------|----------|--------------|
| | | C_{11} | C_{12} | C_{44} | Born's ratio |
| | A° | units of 10^{11} dynes/cm ² | | | |
| Gallium Arsenide | 5.6535 ^a | 11.81 ^b | 5.32 | 5.94 | 0.945 |
| Gallium Phosphide | 5.4506 ^a | 13.75 ^c | 6.32 | 6.84 | 0.944 |
| Indium Antimonide | 6.4789 ^a | 6.67 ^d | 3.65 | 3.02 | 0.914 |
| Indium Phosphide | 5.8688 ^a | 10.22 ^e | 5.76 | 4.60 | 0.902 |
| Aluminium Antimonide | 6.1356 ^a | 8.939 ^f | 4.427 | 4.155 | 0.957 |

a) Giesecke, G. and Pfister, H., Acta Cryst., 11, 369 (1958).

b) Garland, C.W. and Park, K.C., J. Appl. Phys. 33, 757 (1962).

c) Estimated here.

d) Slutsky, L.J. and Garland, C.W., Phys. Rev. 113, 167 (1959).

e) Bolef, D.I. and Menes, M., J. Appl. Phys., 31, 1426 (1960).

Table II

Zone Boundary Frequencies For III-V Compounds.
All frequencies are given in 10^{-2} cm^{-1} units.

| Compounds | | GaAs ^a | GaP ^b | InSb ^c | InP ^d | AlSb ^e |
|--------------------------|----|-------------------|------------------|-------------------|------------------|-------------------|
| Brillouin Zone | | | | | | |
| Σ ₁ [1000] | LO | 8.55 | 11.752 | 6.166 | 10.252 | 10.156 |
| | TO | 8.02 | 11.051 | 5.682 | 9.406 | 9.503 |
| X: [100] | LO | 7.22 | 9.310 | 4.788 | 7.085 | - |
| | LA | 6.80 | 7.931 | 4.280 | 6.915 | - |
| | TO | 7.56 | 10.809 | 5.295 | 8.294 | 8.923 |
| | TA | 2.36 | 3.482 | - | 4.860 | 2.466 |
| L: [111] | LO | 7.15 | 9.866 | 4.812 | 7.544 | 6.988 |
| | LA | 6.26 | 8.367 | 4.087 | 7.109 | 6.432 |
| | TO | 7.84 | 11.317 | 5.392 | 8.923 | 9.189 |
| | TA | 1.86 | 2.055 | 1.306 | 2.611 | 1.862 |

- a) Waugh, J.L.T. and Dolling, G., Phys. Rev., 132, 2410 (1963).
 b) Kleinman, D.A. and Spitzer, W.G., Phys. Rev. 118, 110 (1960).
 c) Franz, S.J., Johnson, F.A. and Jones, R., Proc. Phys. Soc., 76, 939 (1960).
 d) Stierwalt, D.L. and Potter, R.F., Proc. Internat. Conf. Phys. Semiconductors, Paper AP-36, 1961.
 e) Turner, W.S. and Reese, W.E., Phys. Rev., 127, 126 (1962).

Table III

Sets of theoretical parameters of SNI model for different III-V compounds. All parameters are given in the units of 10^3 dyn/cm.

| Com- pounds | α | β | μ_1 | μ_2 | ν_1 | ν_2 | χ |
|----------------|----------|---------|---------|---------|---------|---------|--------|
| GaAs | 39.5254 | 34.0 | 4.467 | 3.697 | -4.5 | -4.5 | 3.286 |
| GaP | 44.4853 | 33.0 | -1.161 | 5.7586 | 4.5 | -15.0 | 3.559 |
| InSb | 32.892 | 28.5 | 2.011 | 0.379 | -3.5 | -1.5 | 3.508 |
| InP | 37.3266 | 35.00 | -3.574 | 12.442 | 2.0 | -1.5 | 4.205 |
| AlSb | 30.554 | 29.5 | -1.512 | 6.532 | -3.0 | 1.0 | 2.938 |

Table IV

Sets of theoretical parameters of KS model for the different III-V compounds. All parameters are given in the units of 10^4 dyn/cm.

| Compounds | α_1 | α_2 | $K_1=K_2$ | $L_1=L_2$ | $N_1=N_2$ | G | $\epsilon_1 e$ | $\epsilon_2 e$ |
|-----------|------------|------------|-----------|-----------|-----------|-------|----------------|----------------|
| GaAs | 5.744 | 11.488 | -0.5 | 0 | 0 | 30.78 | 5.55 | 11.63 |
| InSb | 8.305 | 4.152 | -0.5 | -0.5 | 0 | 21.37 | +7.47 | +3.41 |
| AlSb | 4.821 | 9.642 | -0.5 | 0 | 0 | 25.92 | +6.41 | +7.45 |

| Compounds | Ge^2 | H | $h_1 e$ | $h_2 e$ | e^2 | $k_1 e$ | $k_2 e$ |
|-----------|--------|-------|---------|---------|-------|---------|---------|
| GaAs | 2.31 | 20.45 | 5.21 | 10.41 | 1.18 | 1.42 | -0.61 |
| InSb | 2.31 | 13.43 | +2.56 | 0.67 | -0.55 | +0.53 | -1.84 |
| AlSb | 2.31 | 15.38 | +6.14 | +9.43 | 1.50 | +0.56 | +0.80 |

1. Dispersion Curves

Once the parameters are obtained, we substitute these parameters in the expressions for dynamical matrix elements and also we can always insert them into the expressions for special directions (∞) and (∞) for different values of ξ and we will find the dispersion curves given by the following figures (6.1) to (6.10):

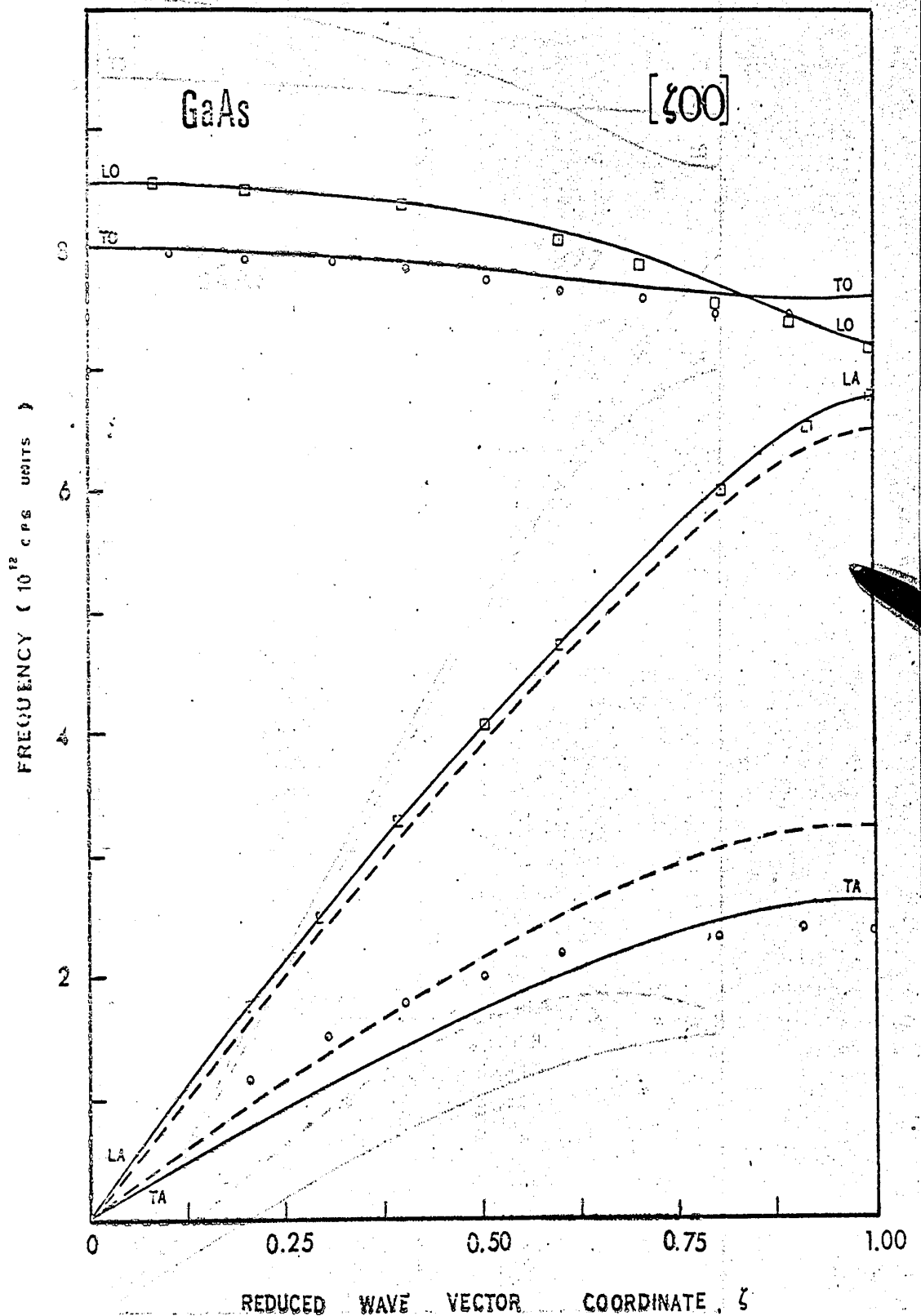


Figure 6.1: Dispersion curves for gallium arsenide in [100] direction. Solid lines denote curves for SNI model, broken line for KS model. Experimental points for longitudinal vibration is shown by □ and transverse by ○.

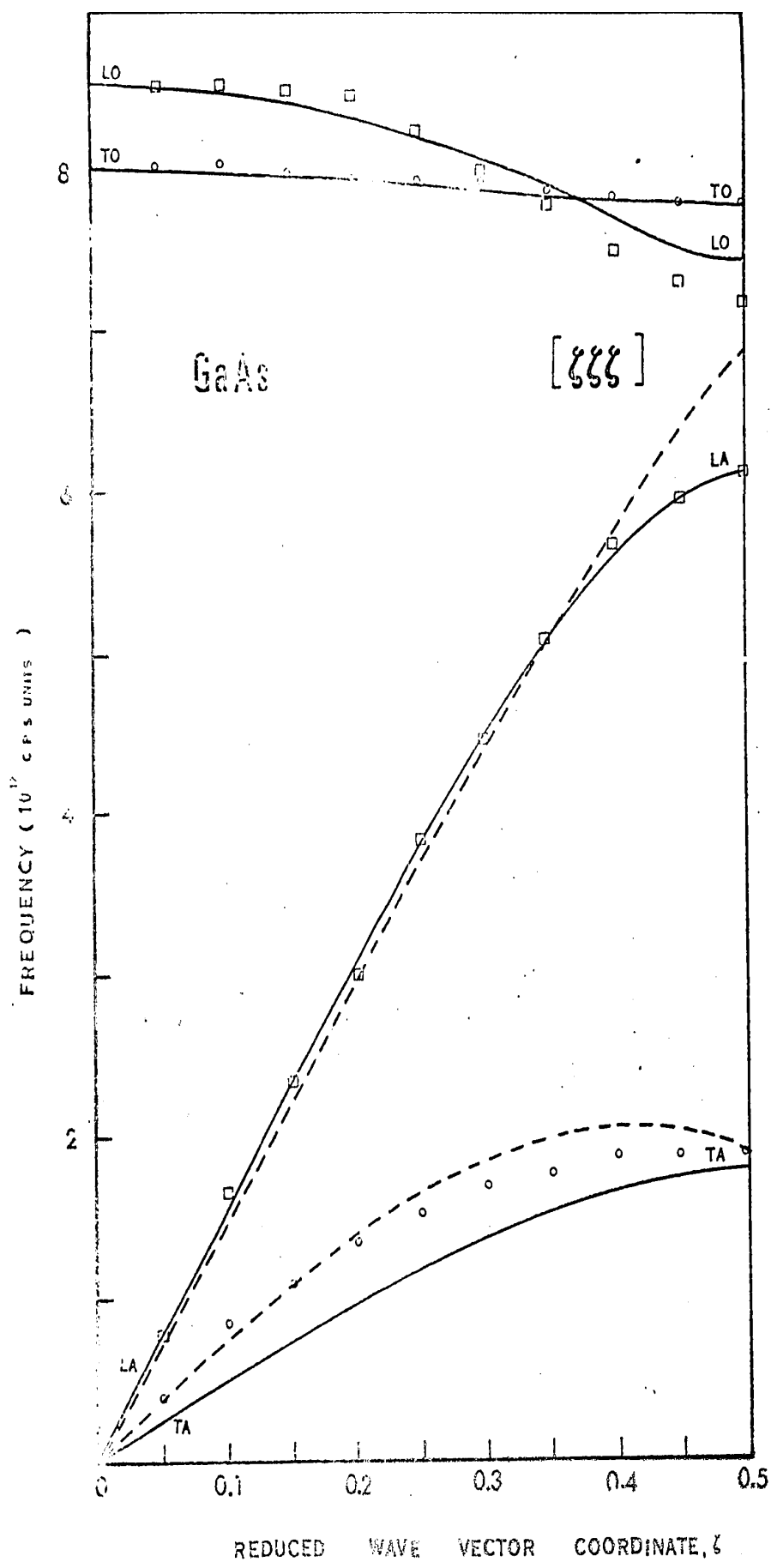


Figure 6.2: Dispersion curves for gallium arsenide in [111] direction. Solid lines denote curves for SNI model, broken line for KS model. Experimental points for longitudinal vibration is shown by \square and transverse by \circ .

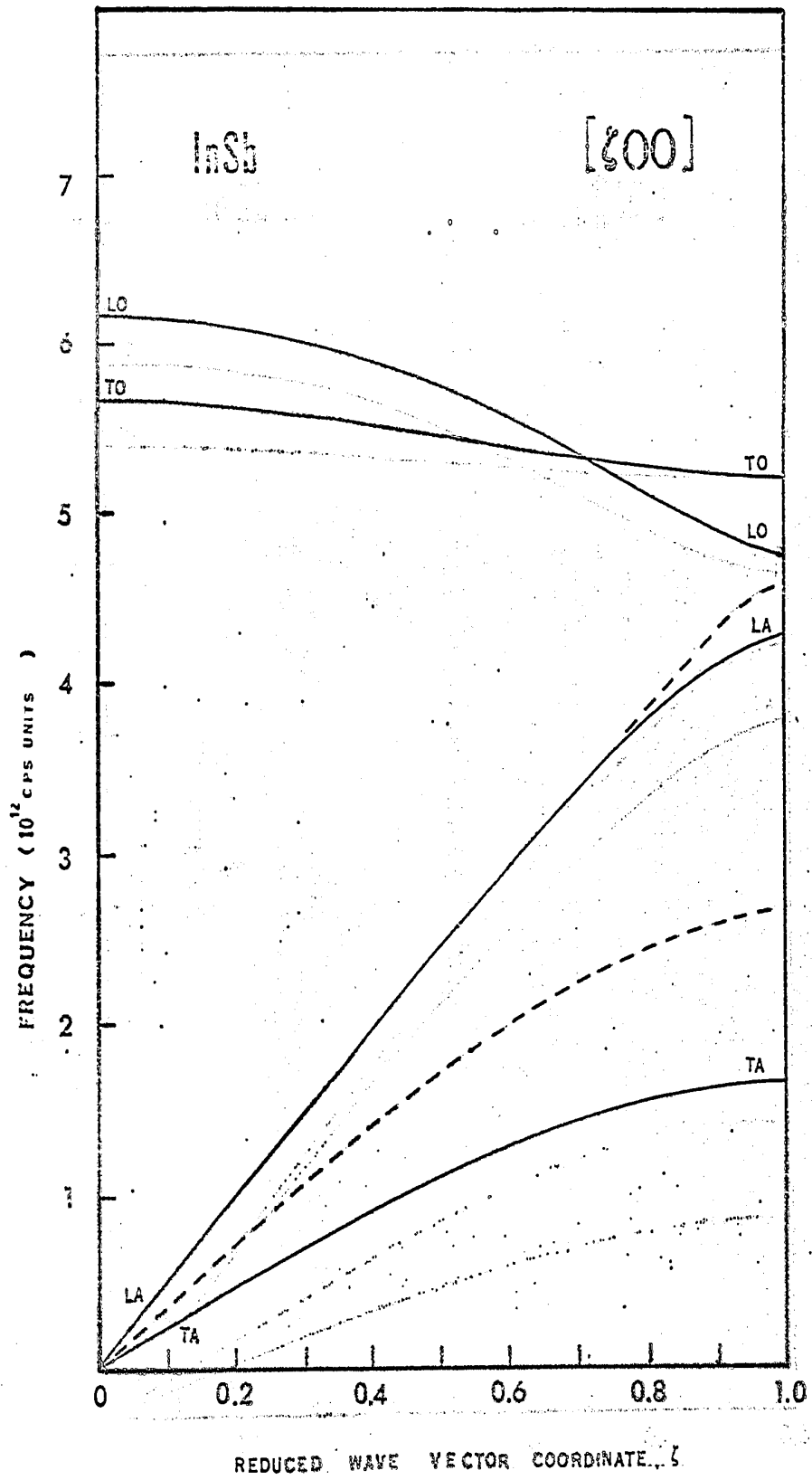


Figure 6.3: Dispersion curves for indium antimonide in [100] direction. Solid lines denote curves for SNI model, broken lines for KS model.

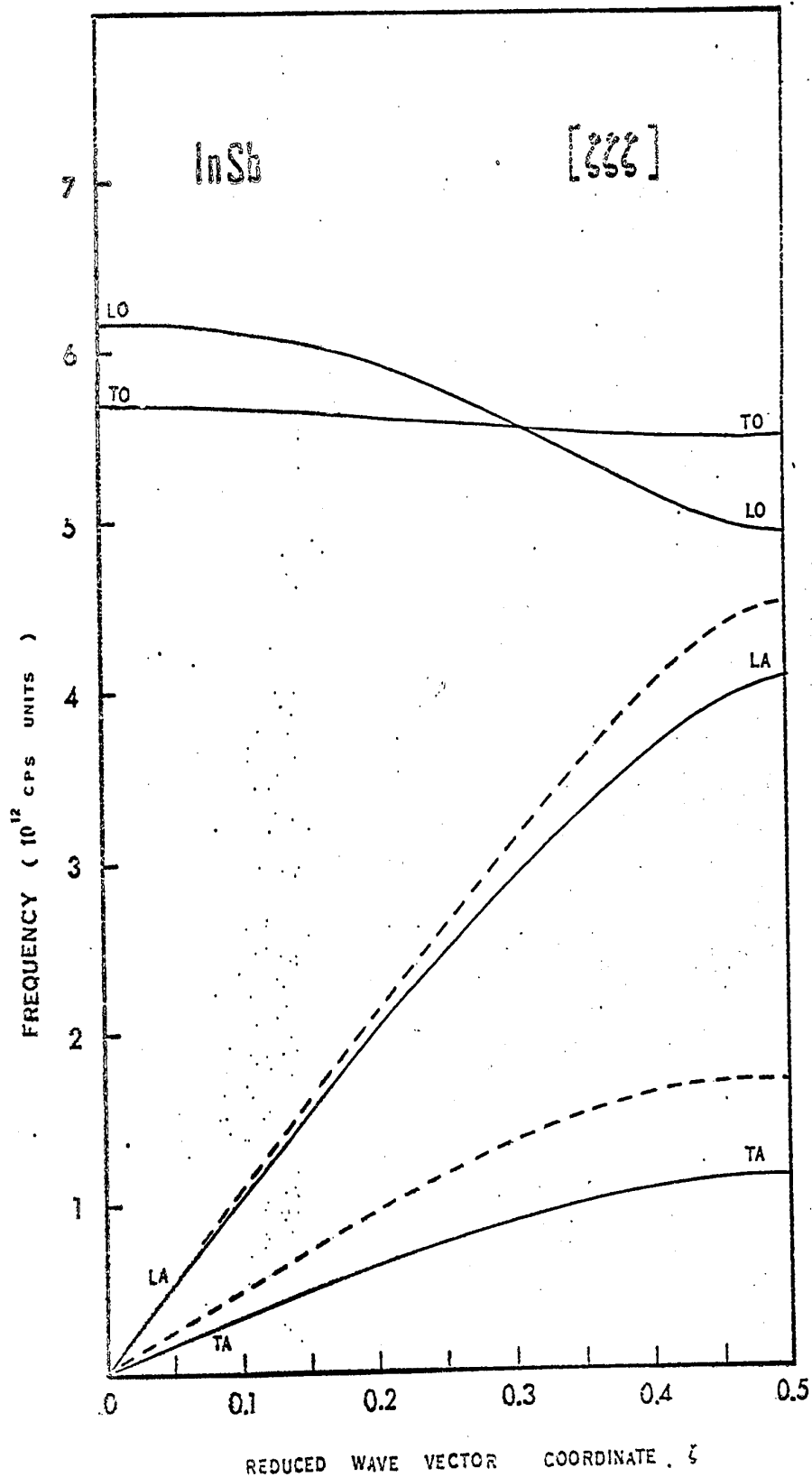


Figure 6.4: Dispersion curves for indium antimonide in [100] direction. Solid lines denote curves for SNI model, broken lines for KS model.

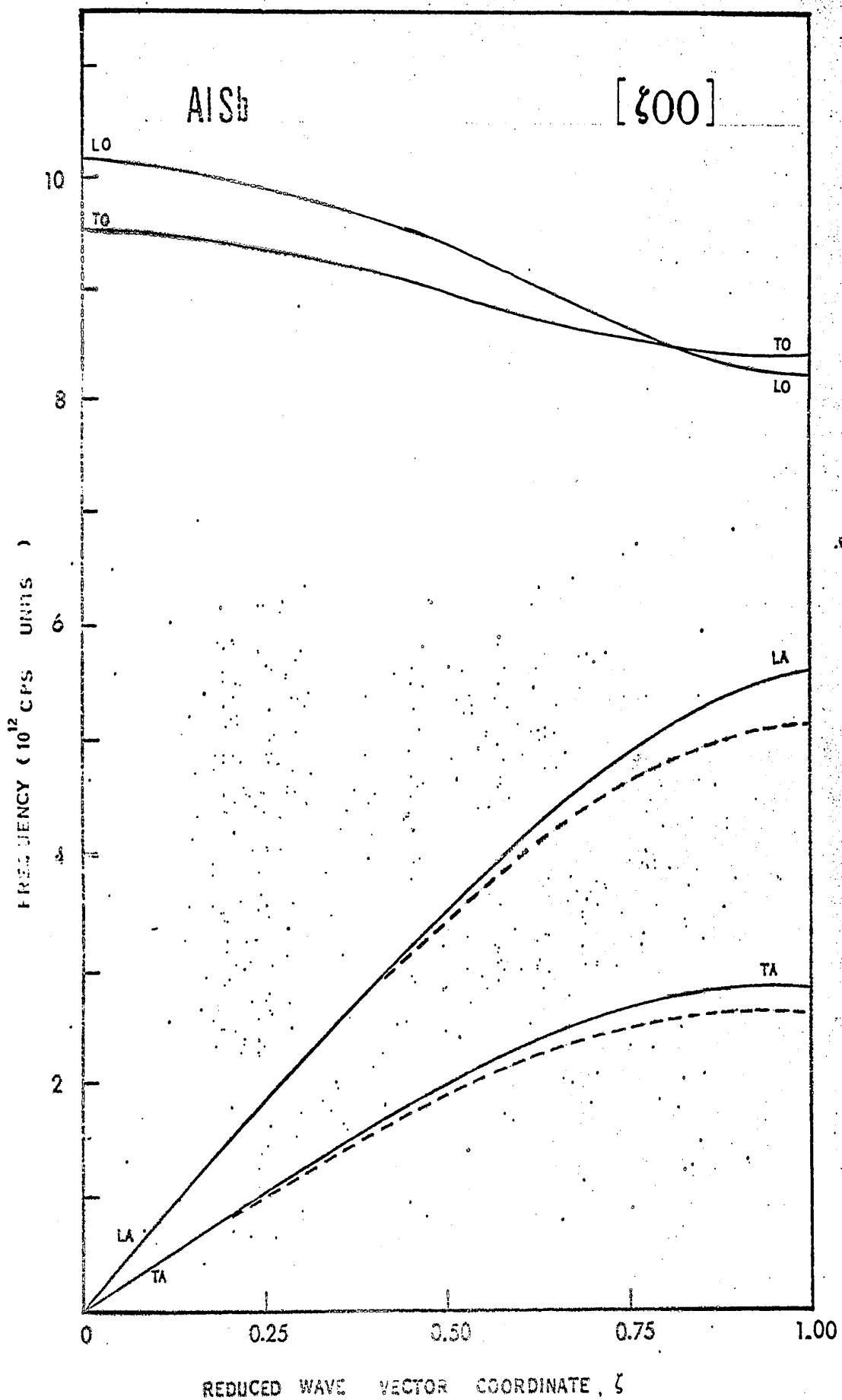


Figure 6.5: Dispersion curves for aluminium antimonide in [100] direction. Solid lines denote the curves of SNI model and the broken lines for KS model.

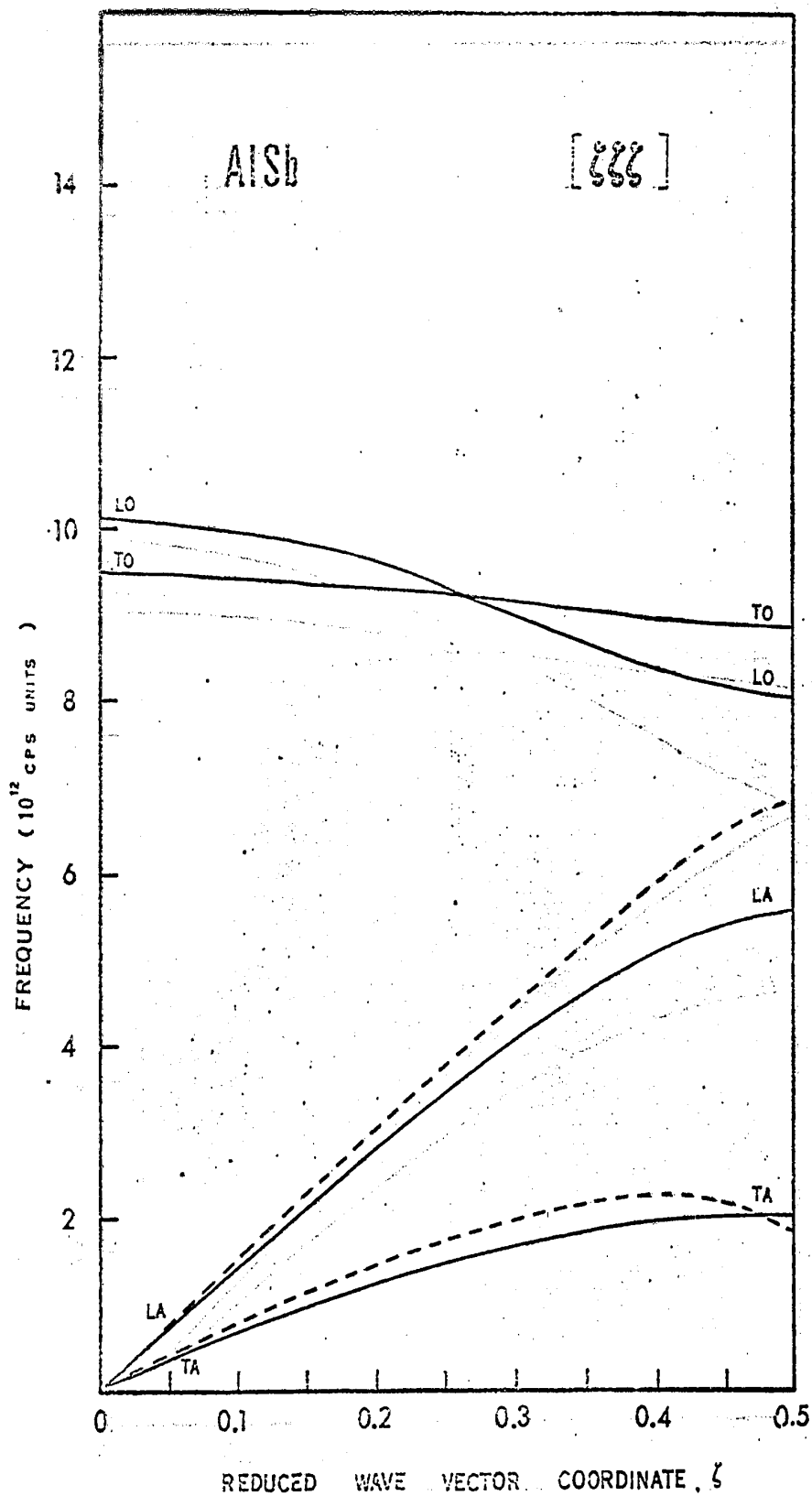


Figure 6.6: Dispersion curves for aluminium antimonide in [111] direction. Solid lines denote the curves for SNI model, broken lines for KS model.

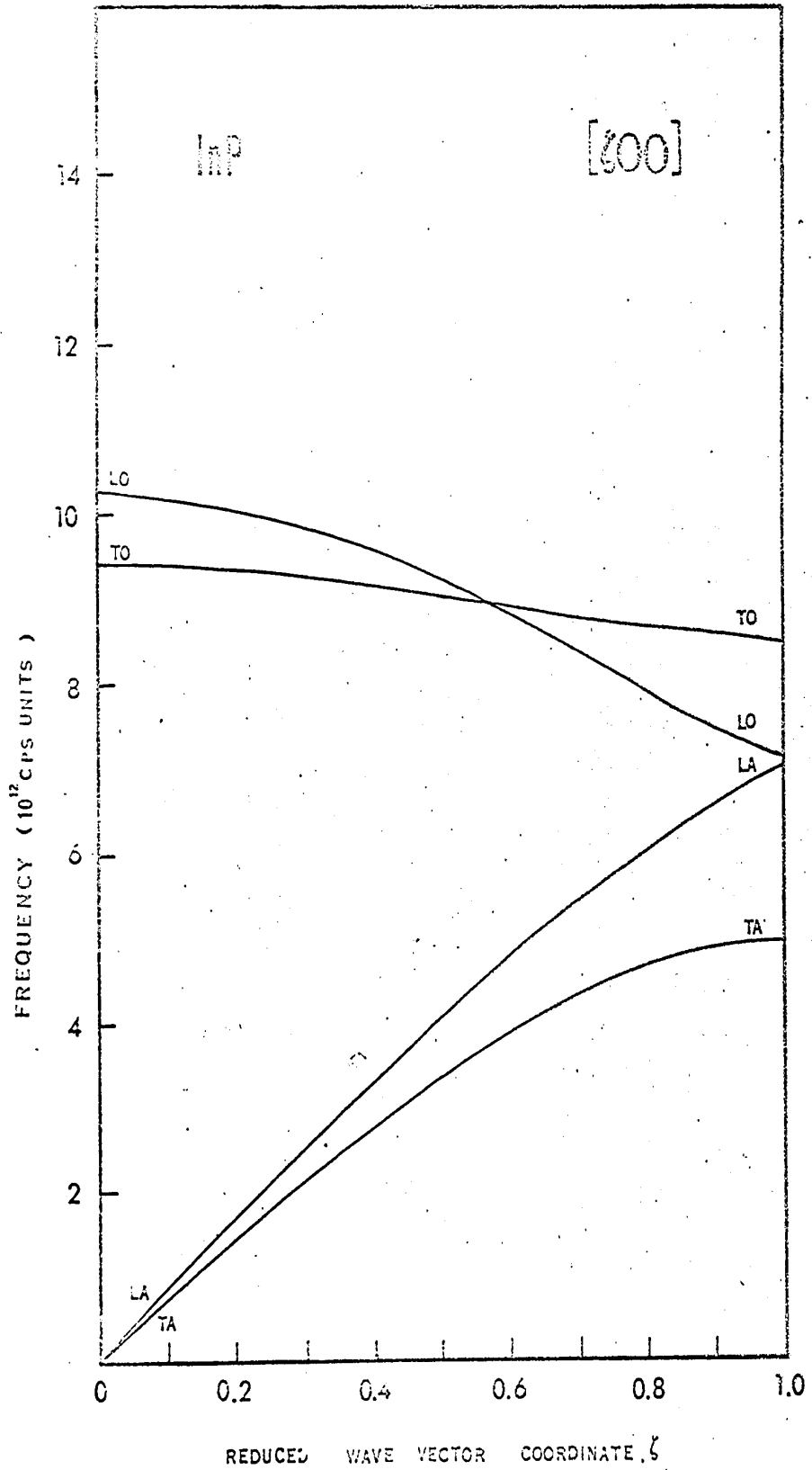


Figure 6.7: Dispersion curves for indium phosphide in [100] direction based on SNI model.

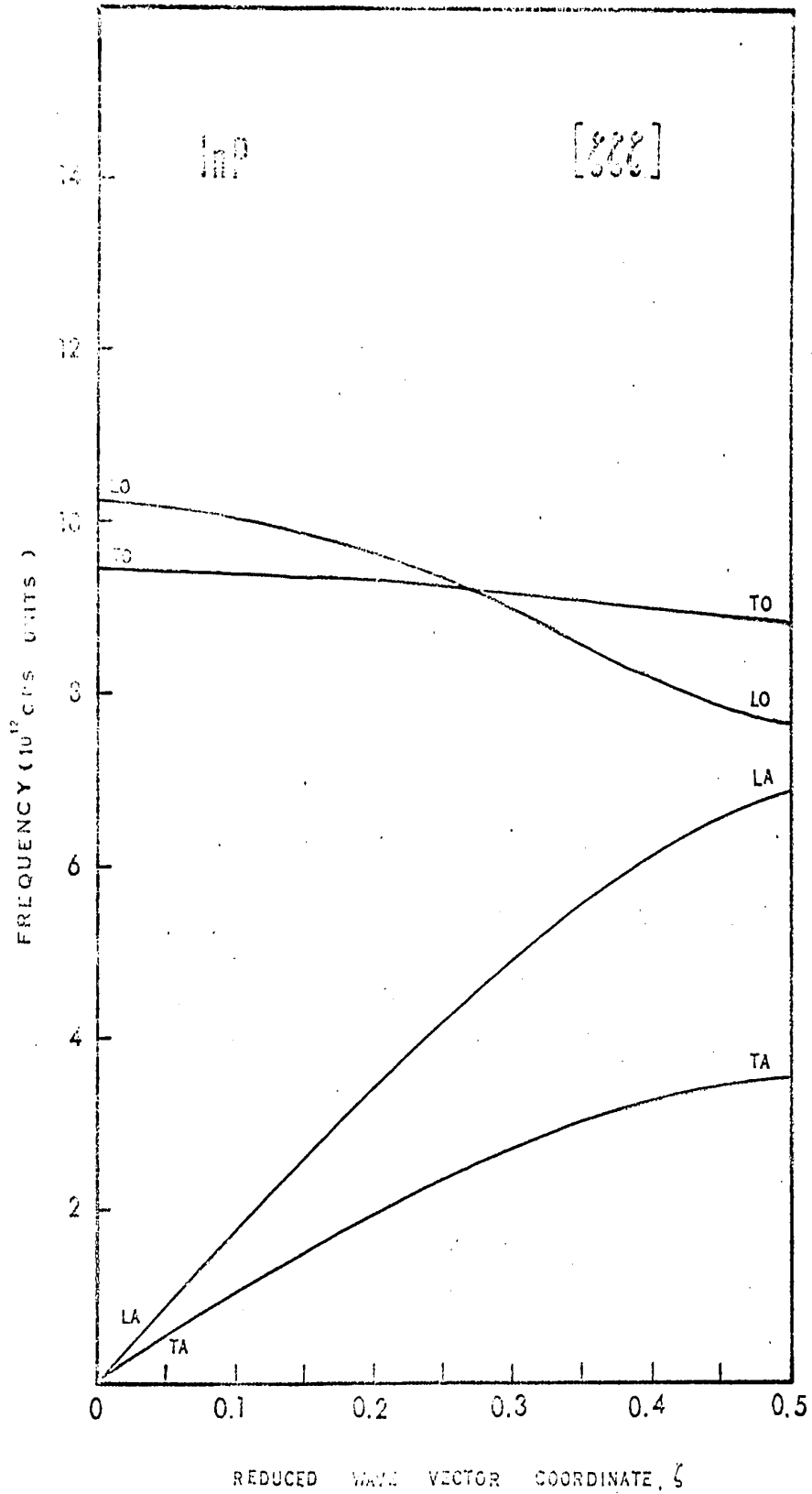


Figure 6.8: Dispersion curves for indium phosphide in [100] direction based on SNI model.

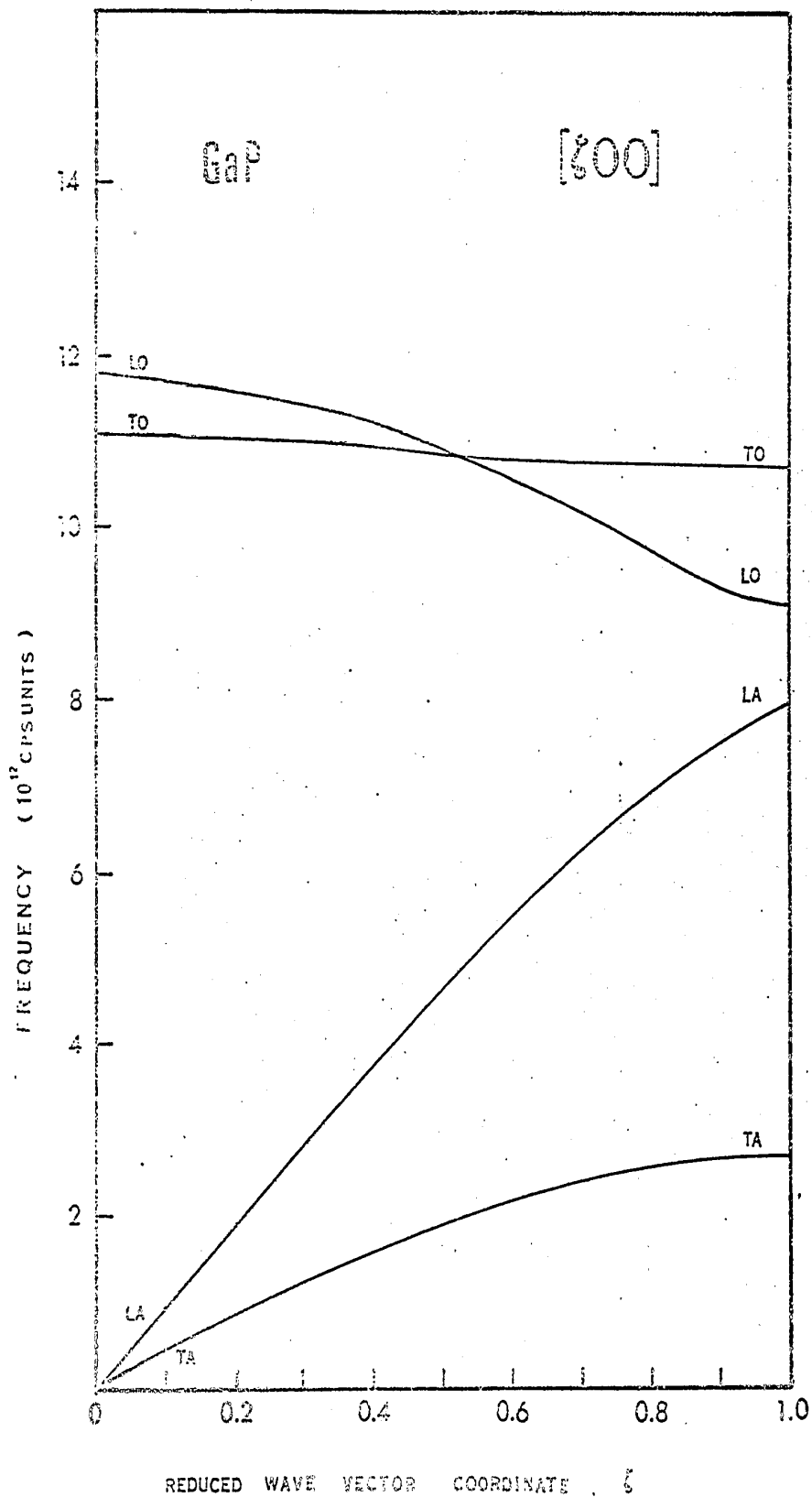


Figure 6.9: Dispersion curves for gallium phosphide in [100] direction based on SNI model.

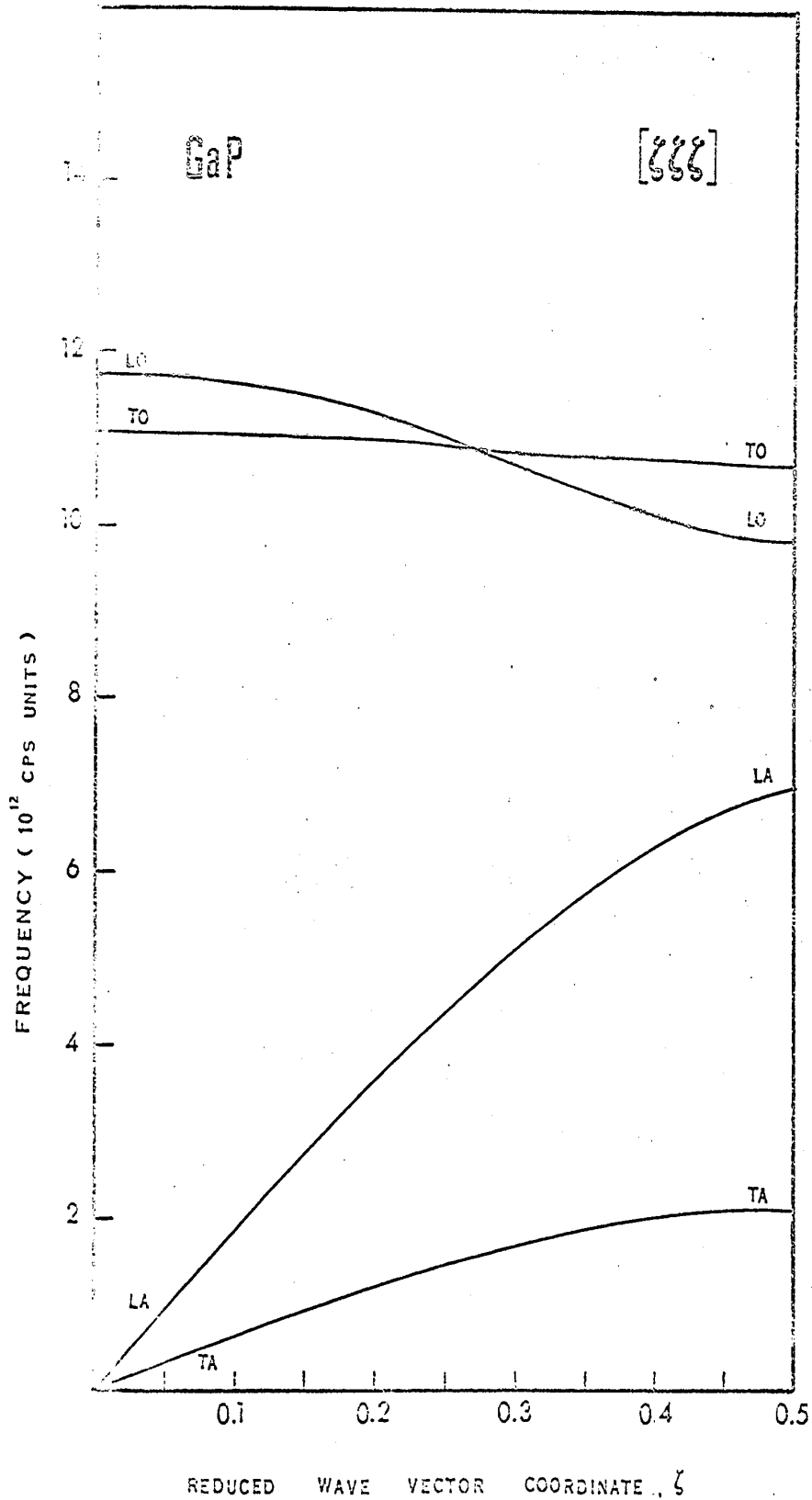


Figure 6.10: Dispersion curves for gallium phosphide in [100] direction based on SNI model.

2. Frequency Spectra

Dispersion curves for special directions can be calculated quite easily since the 6 x 6 matrix which we have to solve for the roots of the secular equation simplifies. But in order to find the frequency spectra we must be able to solve the secular equation in any arbitrary direction. The essential problem is the diagonalization of the dynamical matrix. In the case of 3 x 3 matrix, we can find the roots and that means we can diagonalize quite easily but for matrices of higher rank we have to depend on numerical techniques. One of the methods of diagonalization is Householder's method (AppendixII) which is essentially for symmetric matrix but can be converted to Hermitian matrix too (Blanchard³⁴). IBM 360 computer was used extensively to do the various parts of the numerical calculations.

In order to find $g(v)$ for all these compounds, the reciprocal space was divided into miniature cells with axes one fortieth of the length of the reciprocal

lattice cell. Vibration frequencies were calculated from the roots of the secular determinant for 1686-1 = 1685 wave vectors in the 1/48 of the first Brillouin zone.

The point $\vec{q} = (0, 0, 0)$ was left out because of equations (2.36-2.40). Each point is weighed according to the number of points equivalent to it by symmetry. The total number of points in the whole zone was thus $40^3 - 1 = 63999$, and that of the frequencies $192000 - 6 = 191,994$. The vibration spectra were then constructed using Blackman's sampling technique. The calculation on IBM 360 needs 2 hours to calculate the dynamical matrices and to diagonalize in order to give the roots of the secular equation for all these number of points (see Appendix III for Block diagrams and Flow charts). The vibration spectra thus calculated are given in figures (6.11) to (6.18) for different compounds.

(3) (ARBITRARY UNITS)

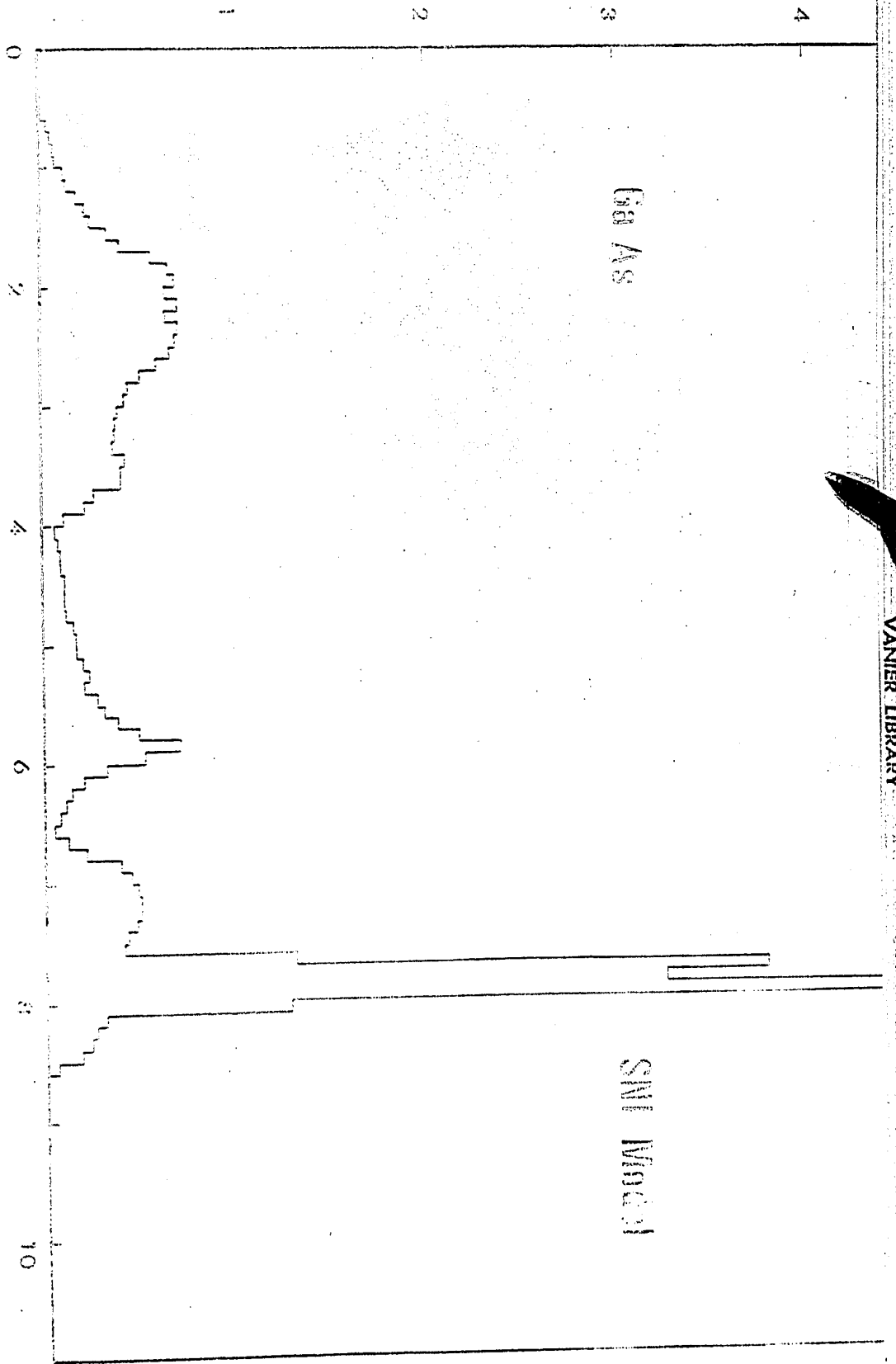


Figure 5.11: Histogram for frequency distribution of Ga As and SMI Model.

(2) ARBITRARY UNITS

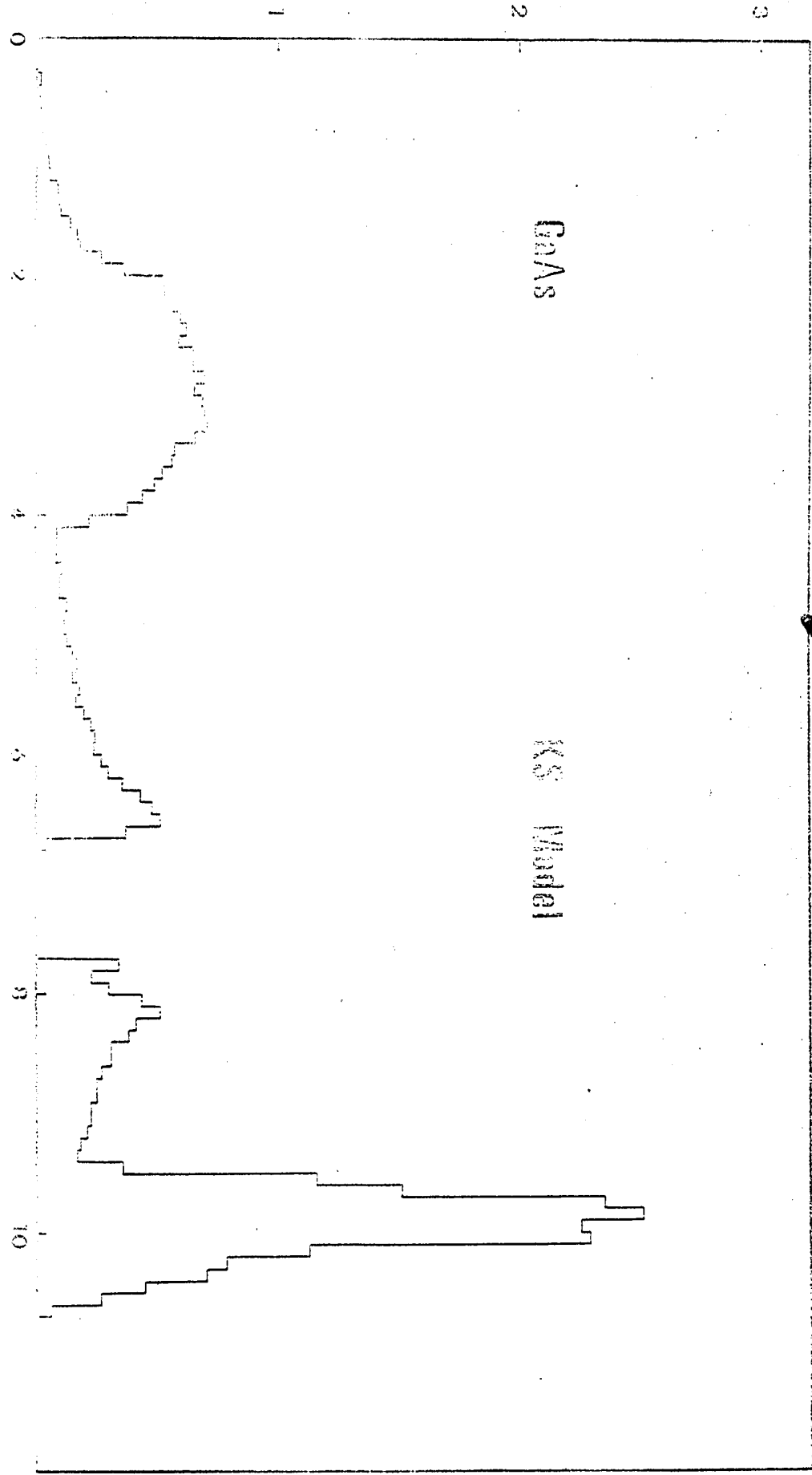
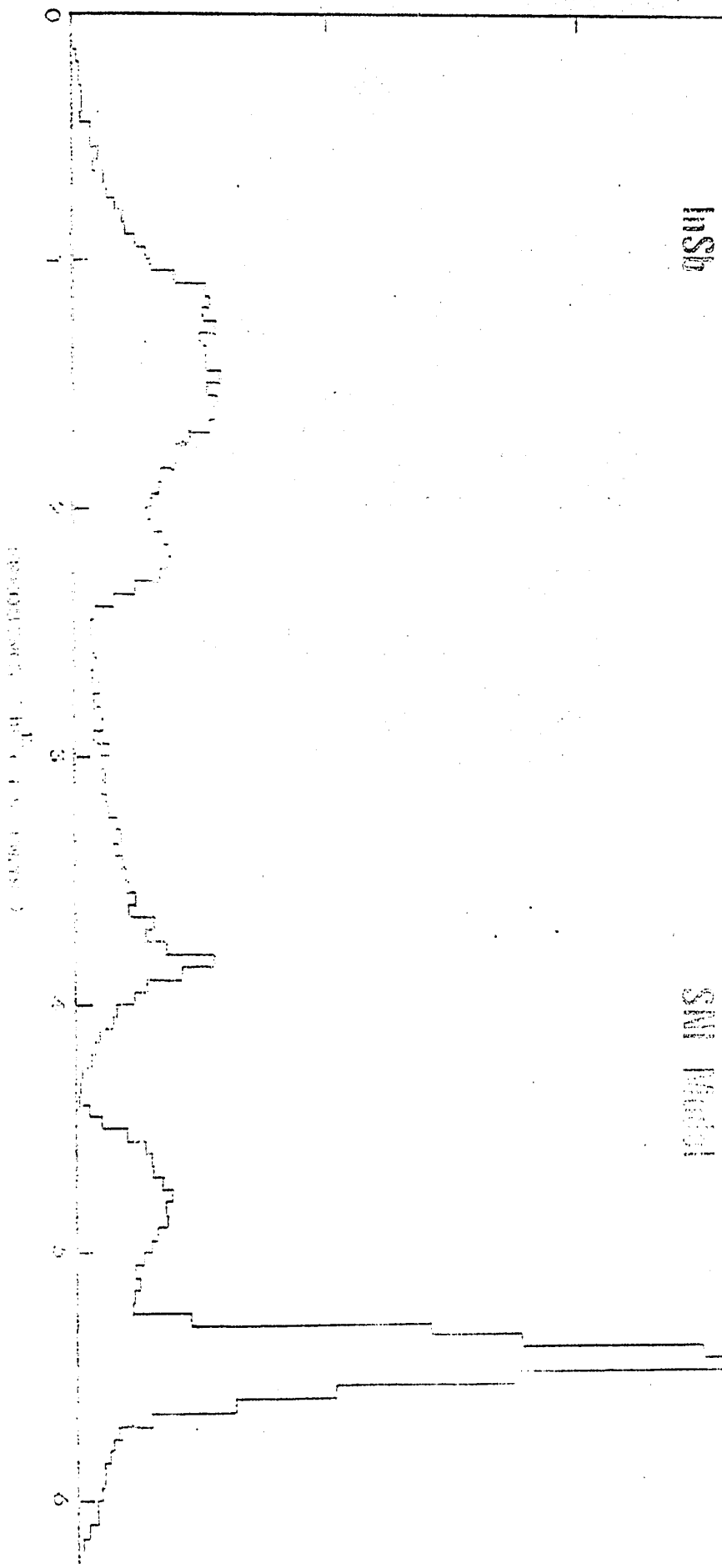


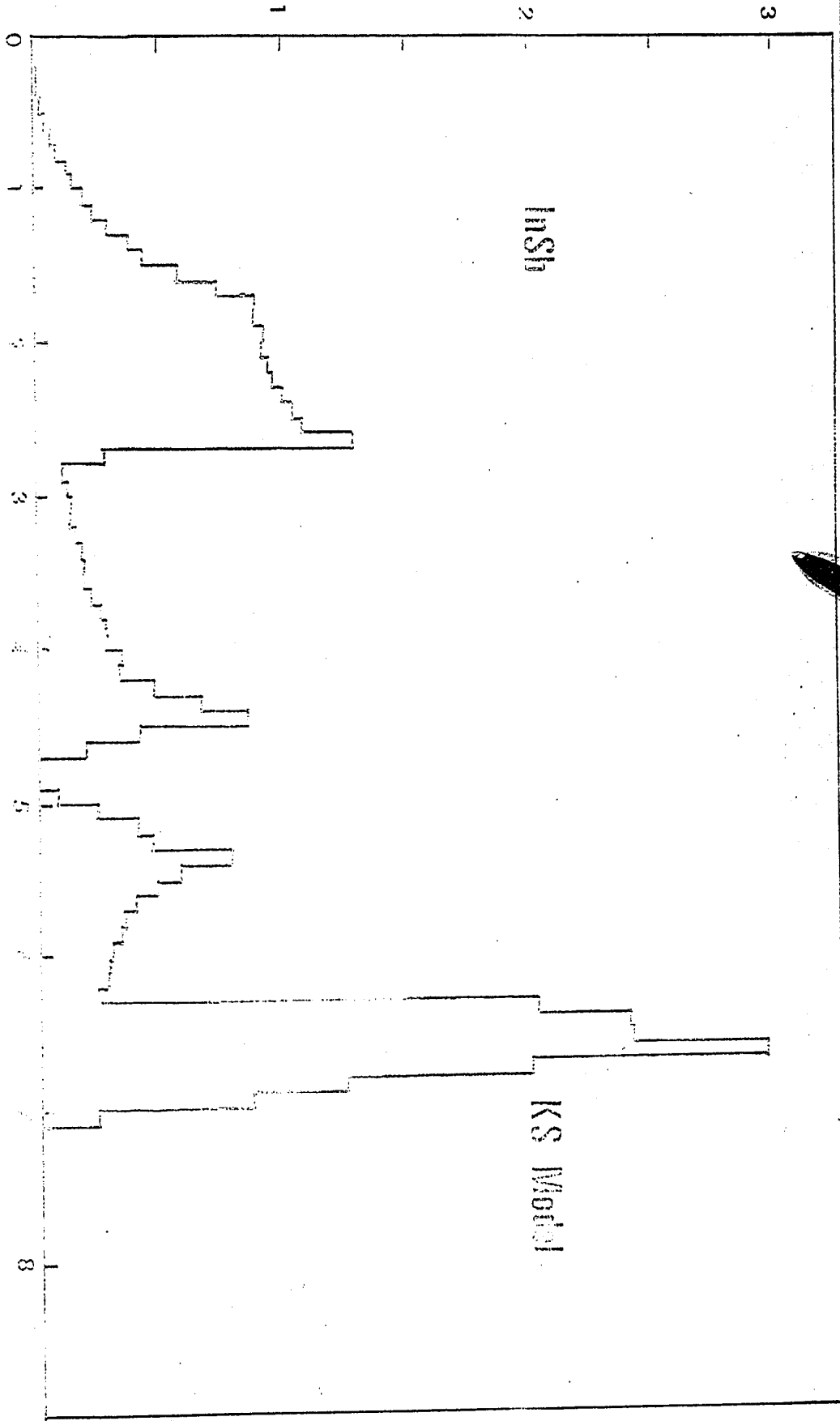
FIGURE 1
 Comparison of the frequency distribution of the number of operations per second for the Gas and KS Model.

$y(\nu)$ (ARBITRARY UNITS)

Figure 6.13 Histogram for frequency distribution function computed for random sequence data based on SMI



$g(\nu)$ (ARBITRARY UNITS)



FREQUENCY (10¹² cps. band)
 Comparison of the frequency distribution of the observed data with the KS Model.

Figure 1. Comparison of the frequency distribution of the observed data with the KS Model.

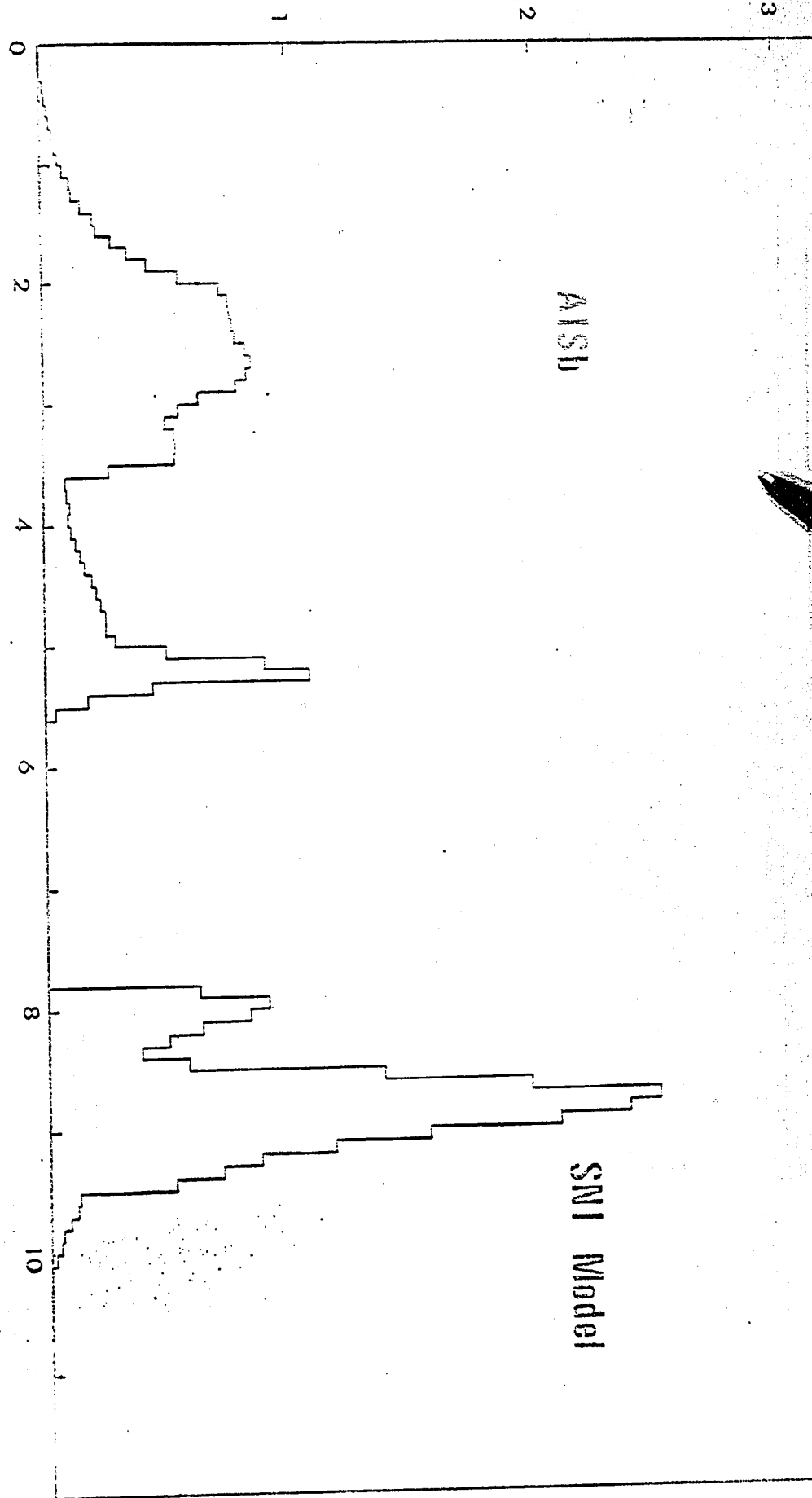


Figure 6.5: Histograms of Frequency Distribution Function
 of AISB and SNI Model. The SNI Model is based on SNI model.

CONFIDENTIAL

$g(\nu)$ (ARBITRARY UNITS)

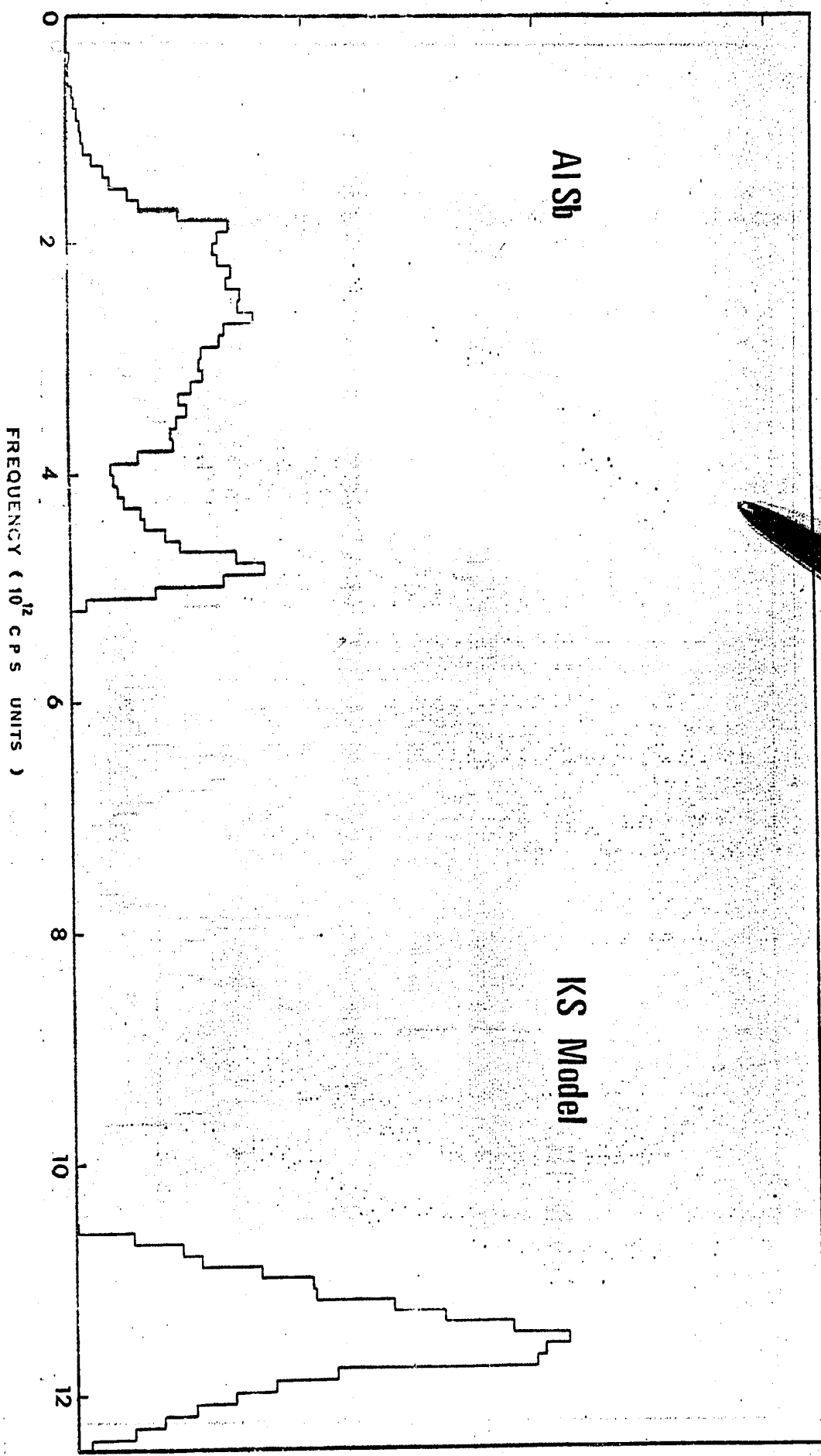


Figure 6.16: Histogram for frequency distribution function computed for simulating antimonide based on KS model.

[(v)] [ARBITRARY UNITS]

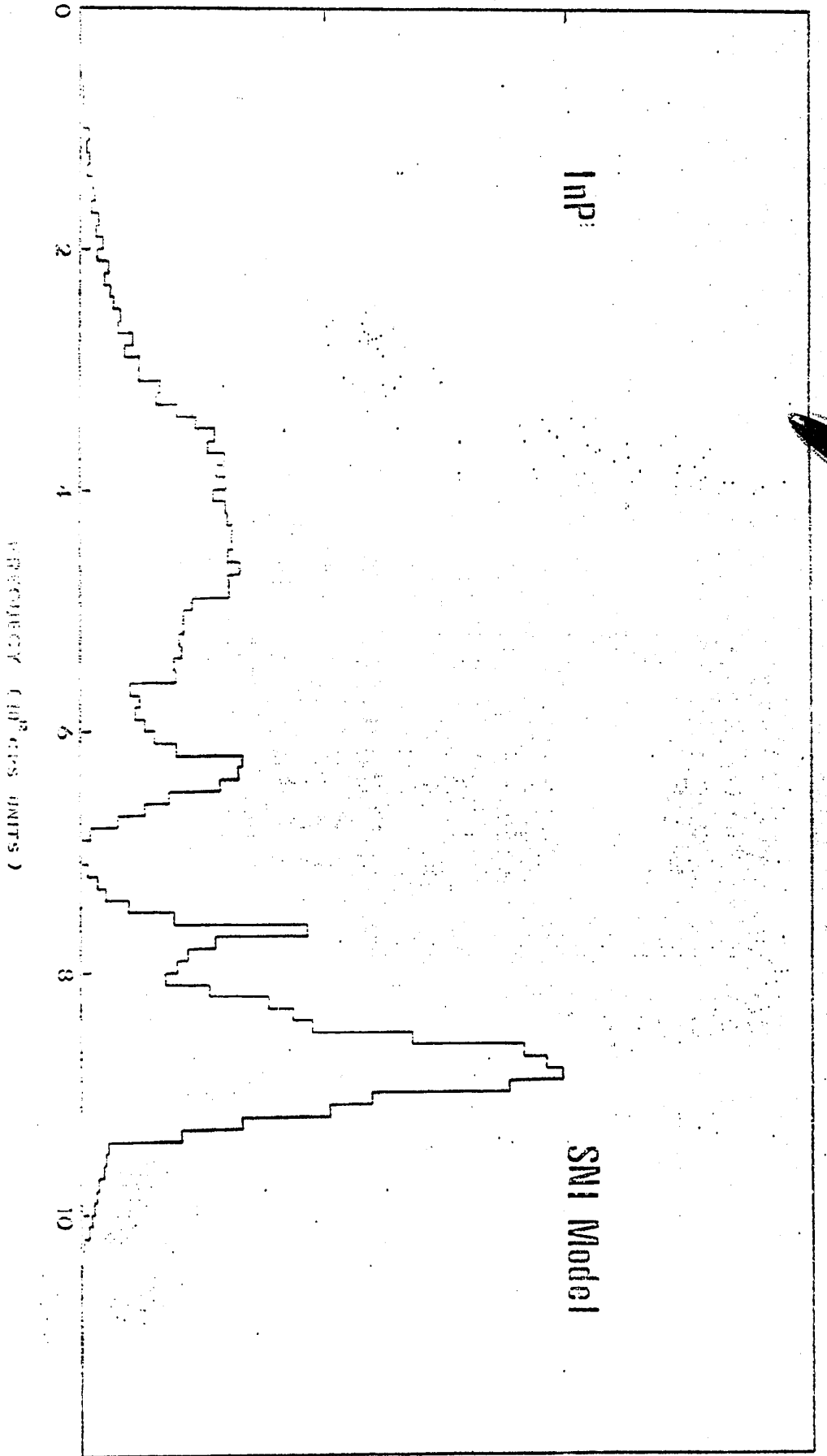


Figure 6.17: InP and SNI Model comparison. The data shown is based on SNI model.



$\rho(\nu)$ (ARBITRARY UNITS)

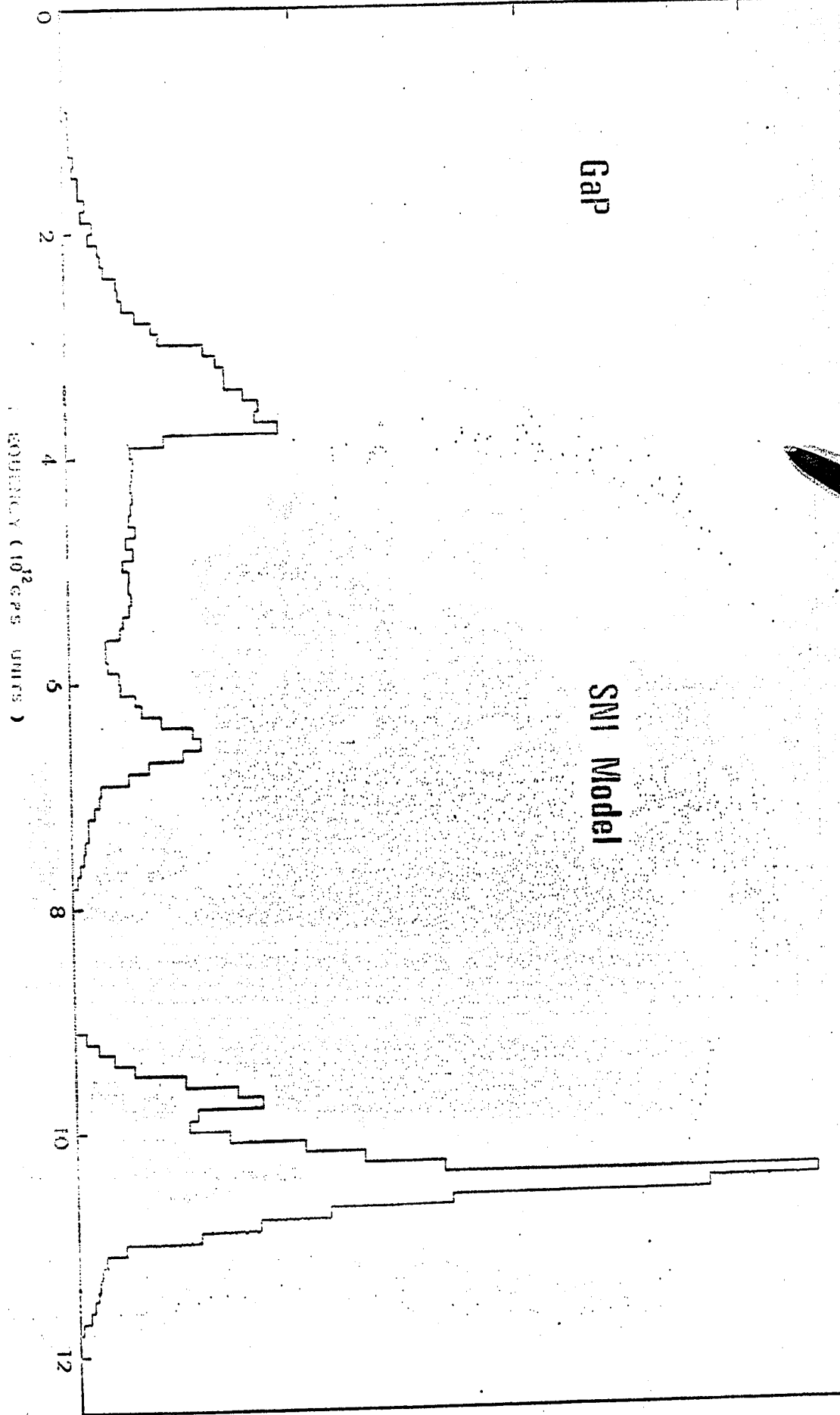


Figure 6.18: Histogram for frequency distribution computed for Gallium phosphide based on SMI model.

3. Obtaining Debye Θ_D Curve

The specific heat at constant volume is given

by

$$C_V = 3R \int_0^{\nu_m} \frac{x^2 e^x}{(e^x - 1)^2} g(\nu) d\nu \quad (6.1)$$

where $x = \frac{h\nu}{kT}$

and

$$\int_0^{\nu_m} g(\nu) d\nu = 1 \quad (6.2)$$

the equivalent Debye temperature Θ_D was calculated from

these equations and they are given in the fig. (6.19) to (6.23).

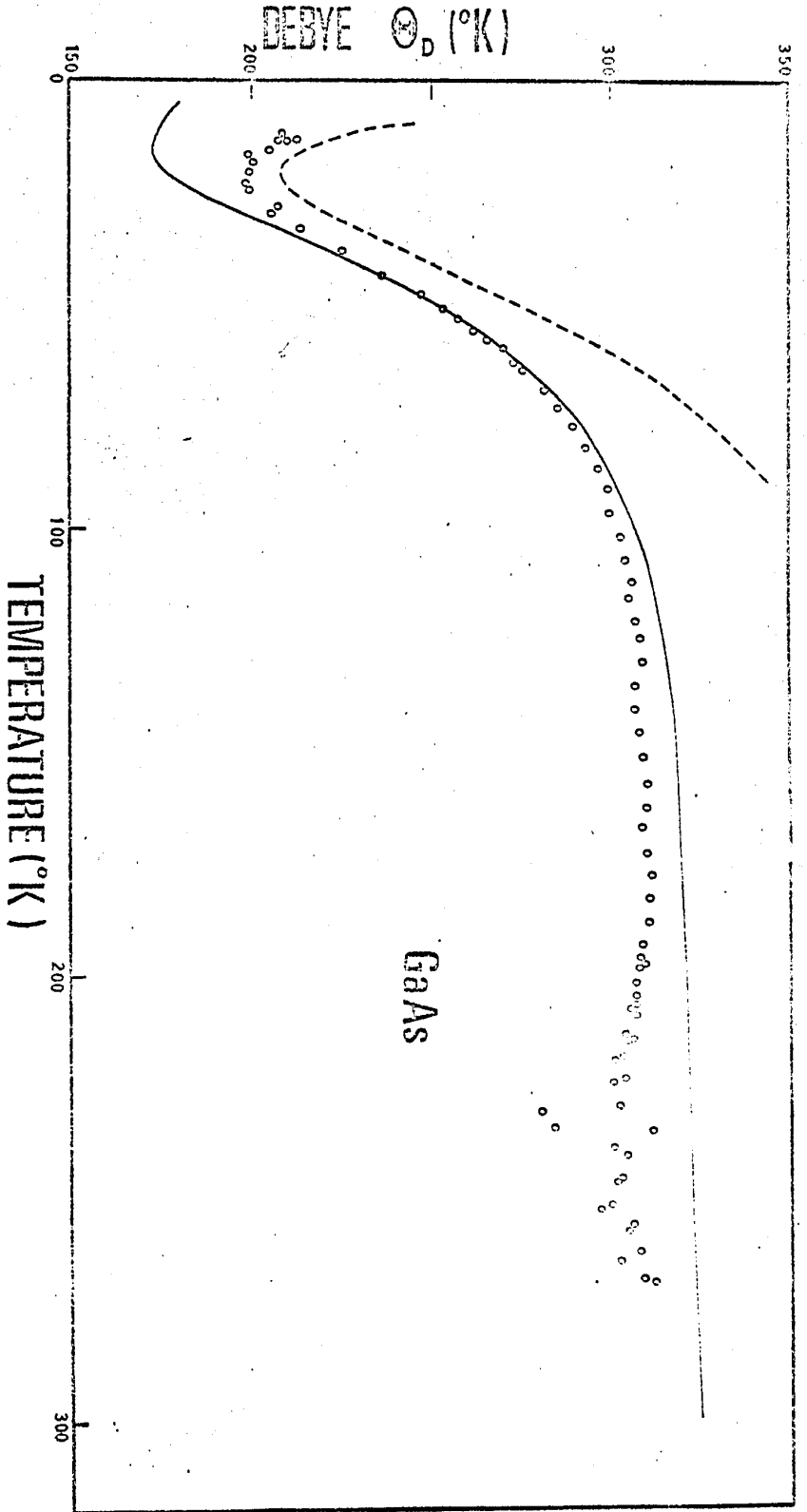


Figure 6.19: Variation of Debye temperature θ_D , with temperature for gallium arsenide. The full curve shows the calculations based on SNI model, the broken curves show the calculations based on KS model, the experimental points are from Plesbergen's paper.

1955
 12
 1955
 the
 these

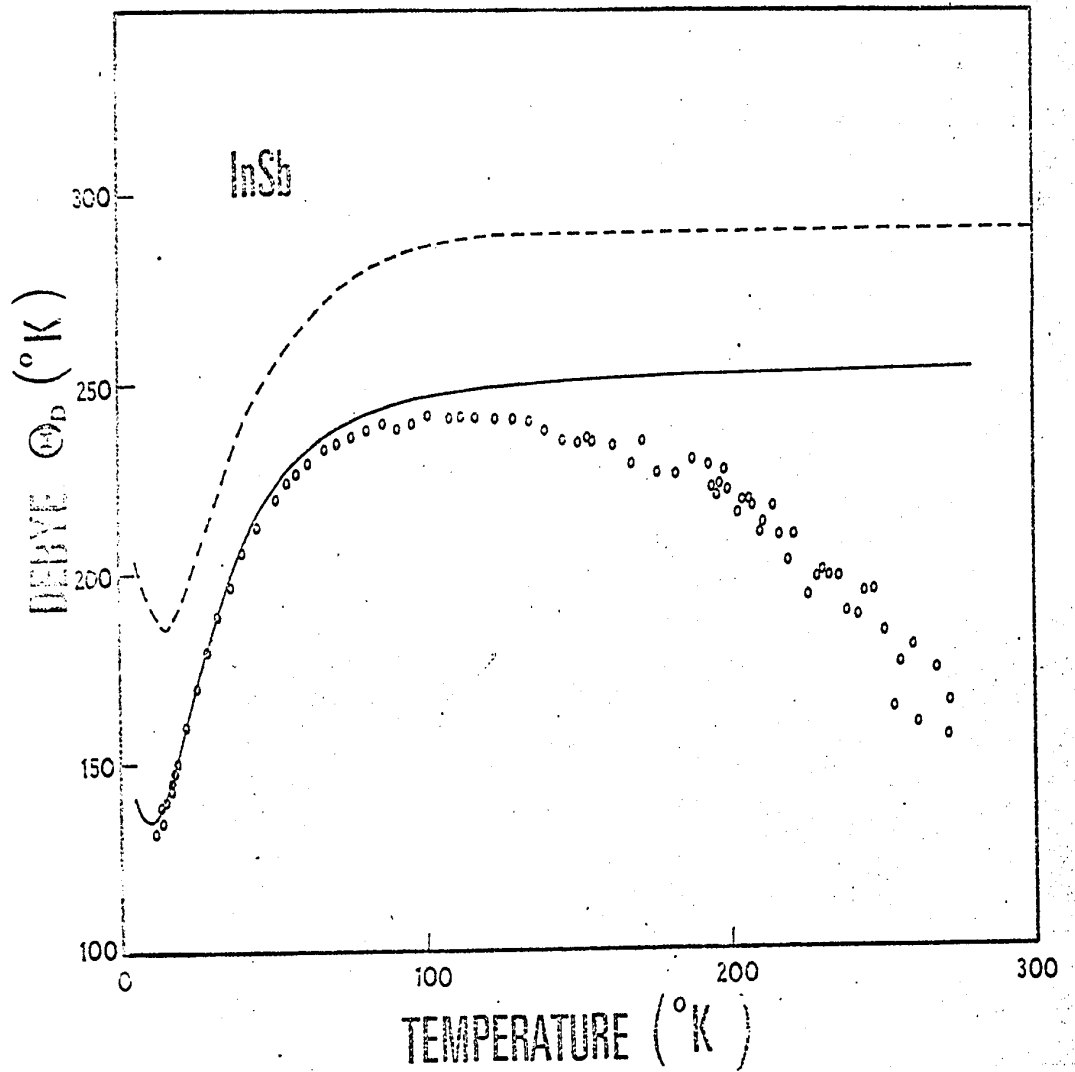


Figure 6.20: Variation of Debye temperature Θ_D , with temperature, for indium antimonide. The full curve shows the calculations based on SNI model, the broken curves show the calculations based on KS model, the experimental points are taken from Piesbergen's paper.

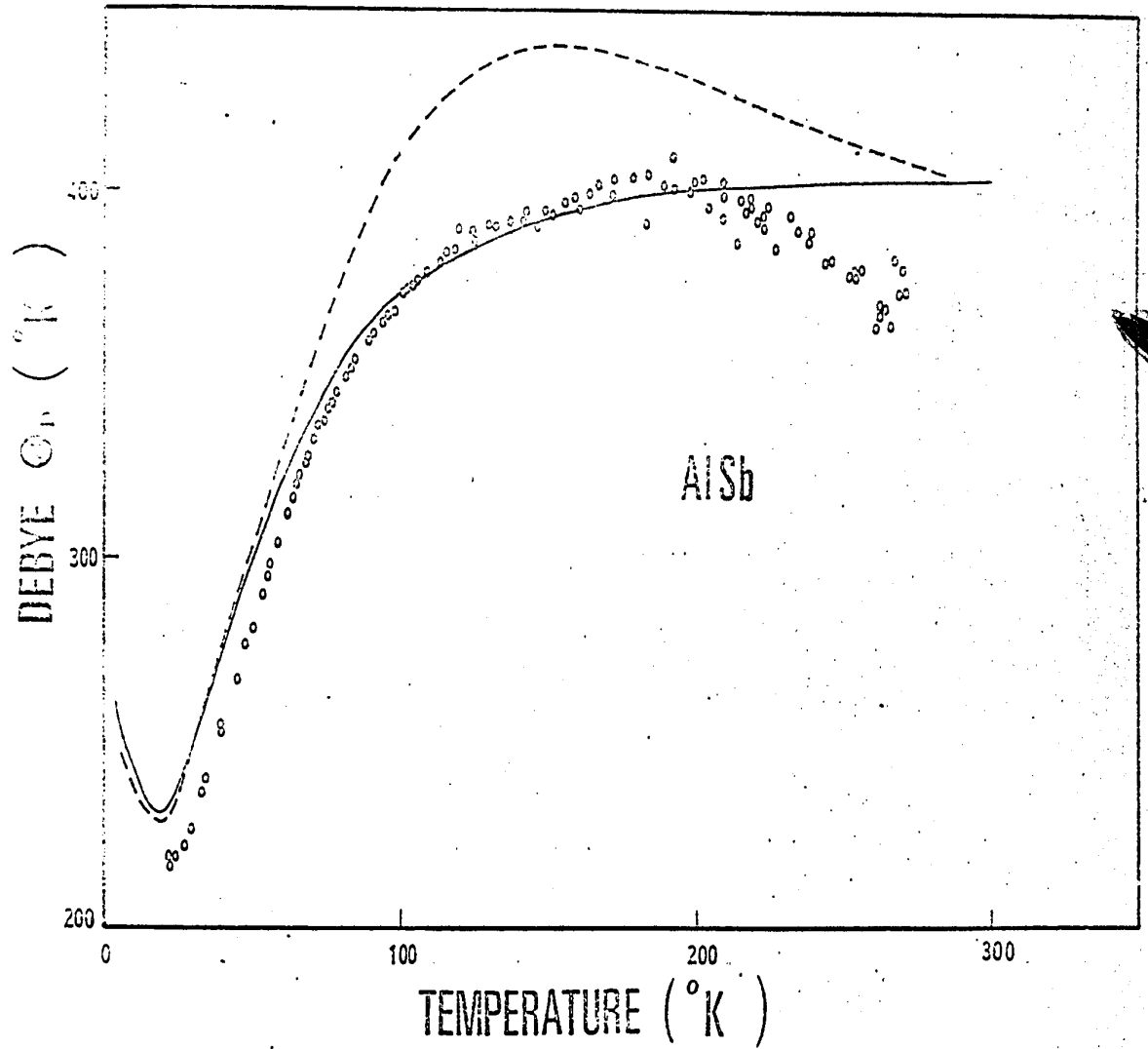


Figure 6.21: Variation of Debye temperature Θ_D , with temperature, for aluminium antimonide. The full curve shows the calculations based on SNI model, the broken curves are based on KS model, the experimental points are taken from Piesbergen's paper.

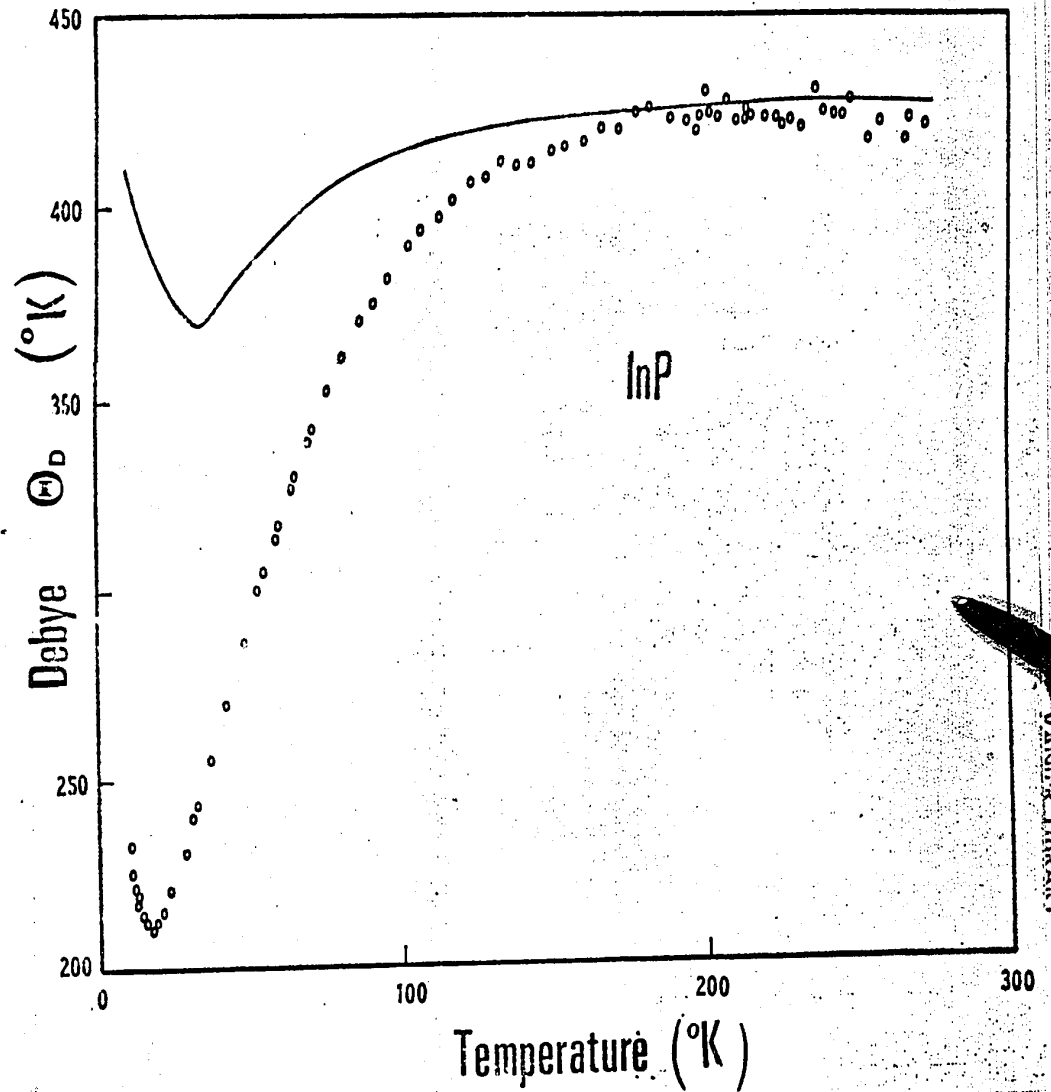


Figure 6.22: The variation of Debye temperature Θ_D , with temperature, for indium phosphide. The curve shows the calculations based on SNI model, while the points denote the experimental points.

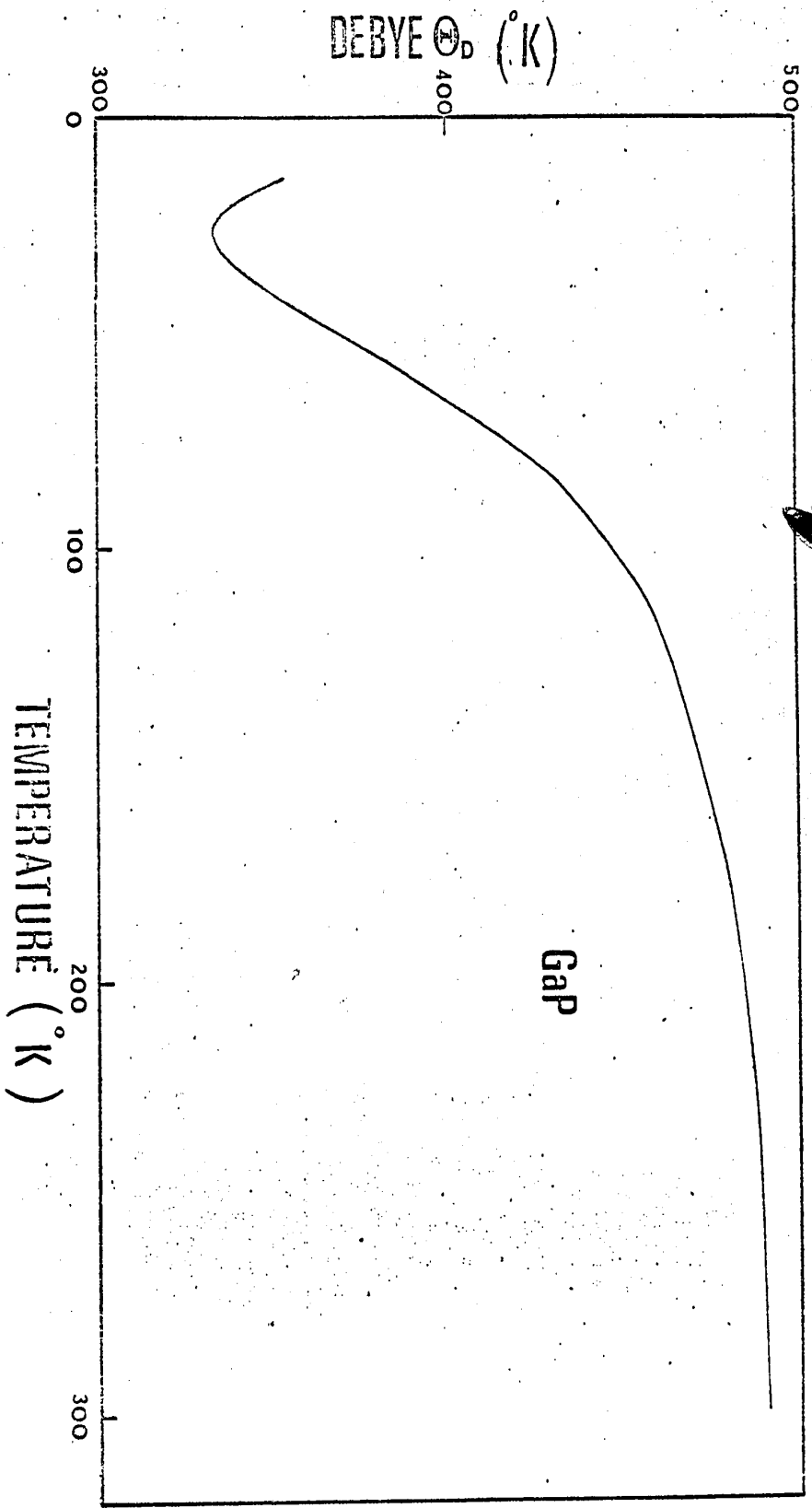


Figure 6.23: The variation of Debye temperature Θ_D , with temperature, for gallium phosphide. The curve shows the calculations based on SNI model.

(1) 6.23

CHAPTER VII

DISCUSSIONS

Except for gallium arsenide, other III-V compounds considered here have only a limited amount of experimental data available. Thus, the results must be discussed more for the general behaviour of the theoretical model than for the quantitative agreement with the experimental results. For gallium arsenide, sufficient data on dispersion curves are available. A reasonable amount of data is also available for Debye ϵ of these compounds. We discuss mainly the following four aspects:

- 1) The choice of the parameters in consideration of their satisfying the elastic constant equations and obtaining the dispersion curves.
- 2) Frequency spectra.
- 3) Debye ϵ curves
- 4) Suitability of the two theoretical models chosen in terms of their explaining the experimental results.

UNIVERSITY LIBRARY

Before discussing the results for individual compounds we would summarize the general features of the various results obtained.

Dispersion curves:

The general characteristics of the dispersion curves follow from the Harmonic lattice theory. Except in KS model for indium antimonide and aluminium antimonide, the acoustic branches increase continuously from zero at [000] of the Brillouin zone to the zone boundary [100] and $[\frac{1}{2} \frac{1}{2} \frac{1}{2}]$. In the optical branch, the frequencies decrease as we go from [000] to either [100] or $[\frac{1}{2} \frac{1}{2} \frac{1}{2}]$, but the relative amount of decrease is smaller than that for the acoustic branch.

Frequency spectra:

On the basis of the Debye theory of specific heat, we should expect $g(\nu)$ as proportional to ν^2 but in general, it is not so and we have for all the compounds a complicated relation between $g(\nu)$ and ν . There are two general properties of the frequency spectra which is

common to all these compounds. Firstly, there is one major peak which is much higher than the other peaks and this lies near the optical zone boundaries and secondly, there are two main regions where most of the frequencies are stacked. The high frequency peak arises from the optical frequencies. Most of the optical frequencies do not change appreciably with the change in the Brillouin zone direction and thus $g(\nu)$ at those frequencies become very large.

Debye ϵ curves:

The experimental results of Piesbergen³⁸ show that the general shape of Debye ϵ curves for III-V compounds are of the same nature as ϵ_D curves for silicon and germanium (Morrison³⁹ et al). If we start from the lowest temperature, ϵ_D first decreases to a minimum, then increases to a flat maximum and finally decreases slowly. Harmonic theory requires that ϵ_D should increase asymptotically with temperature to a constant value ϵ_∞ . This decrease in ϵ_D is to be associated with an anharmonic

VANISIP LIBRARY

effect of a type which cannot be explained by change of volume alone.

Ludwig⁴⁰ (1958) has carried out an extensive theoretical study of the effect of anharmonicity on the properties of crystal lattices. He proposed an additional term in the heat capacity which is directly proportional to the absolute temperature.

Gallium Arsenide:

We have seen, that out of all the compounds we are considering, gallium arsenide has the maximum amount of available experimental data. The elastic constants are well determined experimentally by ultra-sonic pulse-echo technique and the dispersion curves are also known for specific directions from neutron scattering experiments. Thus it is really the best example on which the models proposed can be examined.

Referring to figure 6.1 and 6.2, we find that the dispersion curves for SNI model in both [100] and [111] directions are in good agreement with the experi-

mental results except for the transverse acoustic branch which has a 10% variation. For KS model the optical branches of the curves have very large discrepancies but for acoustic ones the fit is reasonable.

Next we come to the frequency spectra (fig. 6.11 and 6.12). For SNI model, the peak of the spectra is around $8.0 \text{ cps}^{1/2}$ which is within the limits of error of the same peak obtained by Dolling and Cowley, and the general shape is also very similar. KS model gives the peak around $10.0 \text{ cps}^{1/2}$ and a gap in the frequency spectra between $6.8 \text{ cps}^{1/2}$ to $7.7 \text{ cps}^{1/2}$ which are both very unlikely from experimental findings.

For Debye Θ curve (see fig. 6.19), we find that the agreement with the experimental results at low temperatures is reasonable but at high temperatures, due to anharmonic effects, they do not tally so well.

Indium Antimonide:

The dispersion curves are not measured for this compound and hence we only give a qualitative discussion.

We find a good fit in the zone boundary frequencies (see fig. 6.3 and 6.4) for SNI model and the shape of the curves are as expected. For KS model, the acoustic branches resemble well with SNI model but the optical branches are much higher and different from the experimental zone boundary values.

There is a sharp peak at 5.5 cps^{12} in the frequency spectra for SNI model (see fig. 6.13 and 6.14). This peak is shifted to 6.6 cps^{12} in KS model which does not seem reasonable.

For SNI model the behaviour of Debye Θ curve (see fig. 6.20) at lower temperatures is similar to that of gallium arsenide but at higher temperatures, experimental Θ_D decreases rapidly, thus the deviation increases with temperature. It seems that the anharmonic effects in indium antimonide are more dominant than that in gallium arsenide. KS model does not improve the deviation from the experimental results.

* Throughout this discussion, by cps^{12} , we really meant a frequency of 10^{-12} cycles per second for brevity.

Aluminium Antimonide:

The state of things in this compound are almost the same as in indium antimonide. The dispersion curves obtained from the two models in both the directions (see fig. 6.5 and 6.6) are similar to InSb.

Frequency spectra from SNI model has a peak at 8.7 cps^{12} and a gap between the frequencies 5.6 cps^{12} to 7.8 cps^{12} . KS model gives a peak at 11.5 cps^{12} and a gap between 5.3 cps^{12} to 10.5 cps^{12} which is again unlikely (see fig. 6.15 and 6.16).

Debye G curves (see fig. 6.21) based on SNI model coincides well with the experimental data at lower temperatures but fails at higher temperature. KS model gives a good fit at lower temperature but is away at higher temperatures.

Indium Phosphide:

Except for the dispersion curves, all the other experimental data are available now. But the calculation

of the parameters and Debye Θ was done with the help of an estimation of the elastic constants since the elastic constants were not available until very recently.

For SNI model, the zone boundary frequencies have a good fit in both directions (see fig. 6.7 and 6.8). The frequency spectra has a peak at 9.0 cps^{12} .

The theoretical Debye Θ curve is in disagreement with the experimental results. It seems that the zone boundary frequency assignments from the infrared spectra are not correct.

Gallium Phosphide:

In this case, elastic constants or Debye Θ data are not available except for the zone boundary frequencies. Hence the elastic constants were estimated. The zone boundary values in $[555]$ direction coincide reasonably well with the experimental results.

The frequency spectra has a peak at 10.6 cps^{12} and it resembles very much the frequency spectra of GaAs.

The shape of the Debye Θ curve is similar to that of other compounds considered here but since experimental data are lacking, justification for the theoretical model cannot be emphasized.

Comment on the two theoretical models

In SNI model, there is some disagreement in the zone boundary frequencies obtained in $[\xi\xi\xi]$ direction and also in the elastic constants obtained from the parameters chosen. It seems that the assumption $\mu_i = \nu_i$ is not completely satisfactory.

In general, Kaplan and Sullivan's model qualitatively follows the experimental results but the quantitative agreement is poor. We have seen that the dispersion curves for the acoustic branches obtained from KS model are not very different from that obtained from SNI model but the values for the optical branches are significantly different.

For the frequency spectra, KS model, shows the peak at a different place than the frequency expected. Secondly, the gap in the range of frequencies is also larger than expected.

Debye Θ curve obtained from KS model has similar behaviour for very low temperatures but for higher temperature it is very different from the experimental values. The reason for this discrepancy lies in the choice of the parameters. The parameters in their paper should be recalculated.

APPENDIX I

In order to show that the matrix in the second term of the right hand side of eq. (3.6) is hermitian we will show that for a 6 x 6 matrix of similar form as eq. (3.6), the product will be a hermitian matrix.

The matrices of the form

$$C^{CS} = \begin{pmatrix} A & C^* \\ D^* & B \end{pmatrix}; C^{SC} = \begin{pmatrix} A & D \\ C & B \end{pmatrix}; D^{SS} = \begin{pmatrix} E & G^* \\ G & F \end{pmatrix} \quad (A1)$$

where

are all 3 x 3 matrices.

$$\begin{aligned} \begin{pmatrix} A & C^* \\ D^* & B \end{pmatrix} \begin{pmatrix} E & G^* \\ G & F \end{pmatrix} \begin{pmatrix} A & D \\ C & B \end{pmatrix} &= \begin{pmatrix} AE+CG^* & AG^*+CF \\ D^*E+BG & D^*G^*+BF \end{pmatrix} \begin{pmatrix} A & D \\ C & B \end{pmatrix} \\ &= \begin{pmatrix} AE+CG^*A & AED+CG^*D \\ +AG^*C+CF^*C & +AG^*B+CF^*B \\ D^*EA+BGA & D^*ED+BGD \\ +D^*GC+BFC & +DGB+BF^*B \end{pmatrix} \end{aligned} \quad (A2)$$

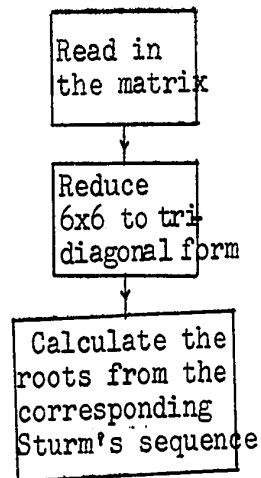
We find that $(AED+CG^*D+AG^*B+CF^*B)$ is the complex conjugate of $(D^*EA+BGA+D^*GC+BFC)$.

This can also be shown for matrices of 6 x 6 order by expanding in detail the terms of the matrix.

APPENDIX II

It was found that the Jacobi method used to diagonalize matrices has a time problem even in IBM 360 and we had to resort to Householder method for determining the Eigenvalues.

The following Block diagram illustrates the scheme of calculations.



Flow Chart 1

This summarizes the Householder's method. He devised a simple rotation matrix which reduces a whole row and column to triple diagonal form in one step.

The post-multiplication by R reduces the row,
the pre-multiplication by R the column.

The first rotation $R'BR$ reduces the first
row and column. After four rotations we get

$$B = \begin{bmatrix} b_1 & c_1 & & & & \\ c_1^* & b_2 & c_2 & & & \\ & c_2^* & b_3 & c_3 & & \\ & & c_3^* & b_4 & c_4 & \\ & & & c_4^* & b_5 & c_5 \\ & & & & c_5^* & b_6 \end{bmatrix}$$

The eigenvalues are then found, using the corresponding
Sturm sequence P_0, P_1, \dots, P_n defined as

$$P_0 = 1$$

$$P_1 = b_1 - x$$

$$P_r = (b_r - x) \cdot P_{r-1} - c_{r-1} c_{r-1}^* P_{r-2} \quad (r = 2, 3, \dots, 6)$$

We illustrate the basic property of this sequence by means
of a simple example.

Consider the 2 x 2 matrix shown below.

$$B = \begin{pmatrix} 1 & i \\ -i & 1 \end{pmatrix}$$

The corresponding Sturm sequence is

$$P_0 = 1$$

$$P_1 = 1 - x$$

$$\begin{aligned} P_2 &= (1 - x) P_1 - (i) (-i) P_0 \\ &= x(x - 2) \end{aligned}$$

We wish to find the eigenvalues of B using Sturm's method.

Firstly take $x = 3$, we get

$$P_0 = 1 \quad +$$

$$P_1 = -2 \quad -$$

$$P_2 = 3 \quad +$$

The number of changes of sign is equal to two. The Sturm property says that there are two roots smaller than $x = 3$.

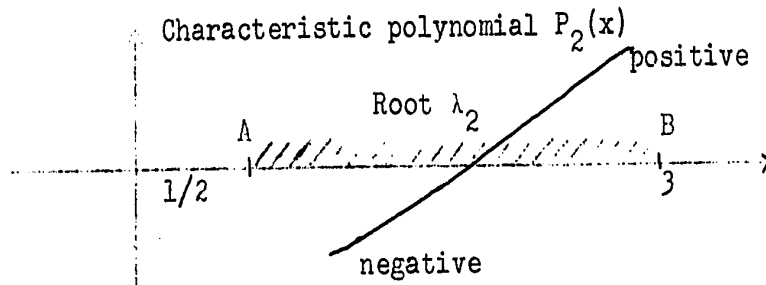
Now trying $x = 1/2$, we get

$$P_0 = 1 \quad +$$

$$P_1 = 1/2 \quad +$$

$$P_2 = -3/4 \quad -$$

There is one change in sign and consequently one root smaller than $1/2$. So we conclude $1/2 < \lambda_2 < 3$.



We now describe the bisection method whereby we can approximate λ_2 to any desired accuracy.

Bisect the hatched interval $(A, B) = (1/2, 3)$ to get $x = 7/4$. Checking the sign of the characteristic polynomial we find that it is negative. So we let $A = 7/4$ and keep $B = 3$. Bisect again to get $x = 19/8$, the characteristic polynomial is now positive, so keep $A = 7/4$ and let $B = 19/8$. In two steps we have found

$$1.75 < \lambda_2 < 2.375 \quad (\text{we know that } \lambda_2 = 2)$$

Speed of convergence: once a root is isolated between A and B , N steps of the bisection method squeezes it within $\epsilon = (B - A)/2^N$. Taking $B - A = 1$ and solving

for N we get $N = \log \epsilon / \log 2$.

Bishop³⁵ and Wilkinson³⁶ give the formulae for a real matrix only. The necessary modifications for a complex matrix can be given in the following way. The rotation matrix is of the form

$$R = I - \mu ZZ'$$

where Z is a column vector, the corresponding row vector being given by

$$Z' = (z_1^*, z_2^*, \dots, z_n^*)$$

and
$$\mu = 1/Z \cdot Z' \tag{A.3}$$

We seek z_1, z_2, \dots, z_n such that the rotation matrix will reduce the matrix B to tridiagonal form by reducing a whole row at a time. The necessary condition is

$$1 = 2 \cdot \mu \cdot \rho\{B\} \cdot Z \tag{A.4}$$

where $\rho\{B\}$ denotes the first row of B

i.e.
$$\rho\{B\} = (b_{1,1}, b_{1,2}, \dots, b_{1,n})$$

and where
$$Z' = (0, z_2^*, b_{1,3}, \dots, b_{1,n})$$

we seek z_2 such that equation (A.4) is satisfied. We re-write (A.4) as follows

$$2P\{B\} \cdot Z = Z \cdot Z' \quad (A.5)$$

Equation (A.5), when written in full, gives

$$2(b_{1,2}z_2 + b_{1,3}b_{1,3}^* + \dots + b_{1,n}b_{1,n}^*) = (z_2^*z_2 + b_{1,3}b_{1,3}^* + \dots + b_{1,n}b_{1,n}^*) \quad (A.6)$$

Since $Z \cdot Z'$ is real, the left hand side of equation (A.6) is real, therefore

$$z_2 = c b_{1,2}^* \quad (A.7)$$

where $c =$ some real constant. Using equation (A.7) we substitute z_2 back into equation (A.6) to get

$$2(c + \chi^2) = c^2 + \chi^2$$

where $\chi^2 = (b_{1,3}b_{1,3}^* + b_{1,n}b_{1,n}^*)/b_{1,2}b_{1,2}^*$. Solving for c we get

$$c = 1 \pm \sqrt{1 + \chi^2} \quad (A.8)$$

Since Z is now determined completely, the rotation matrix is known and we can reduce our matrix B to tridiagonal form.

We now write the formulae for the r^{th} step of the process.

Let \bar{B} stand for the reduced matrix.

Since we want $c = 0$ we select the + sign in equation (A.8)

$$\chi^2 = \left(\sum_{j=r+1}^n b_{r,r+2} b_{r,r+2}^* \right) / b_{r,r+1} b_{r,r+1}^*$$

$$z_j = \begin{cases} 0 & \text{for } j < r+1 \\ b_{r,r+1}^* \left(1 + \sqrt{1 + \chi^2} \right) & \text{for } j = r+1 \\ b_{r,j}^* & \text{for } j > r+1 \end{cases}$$

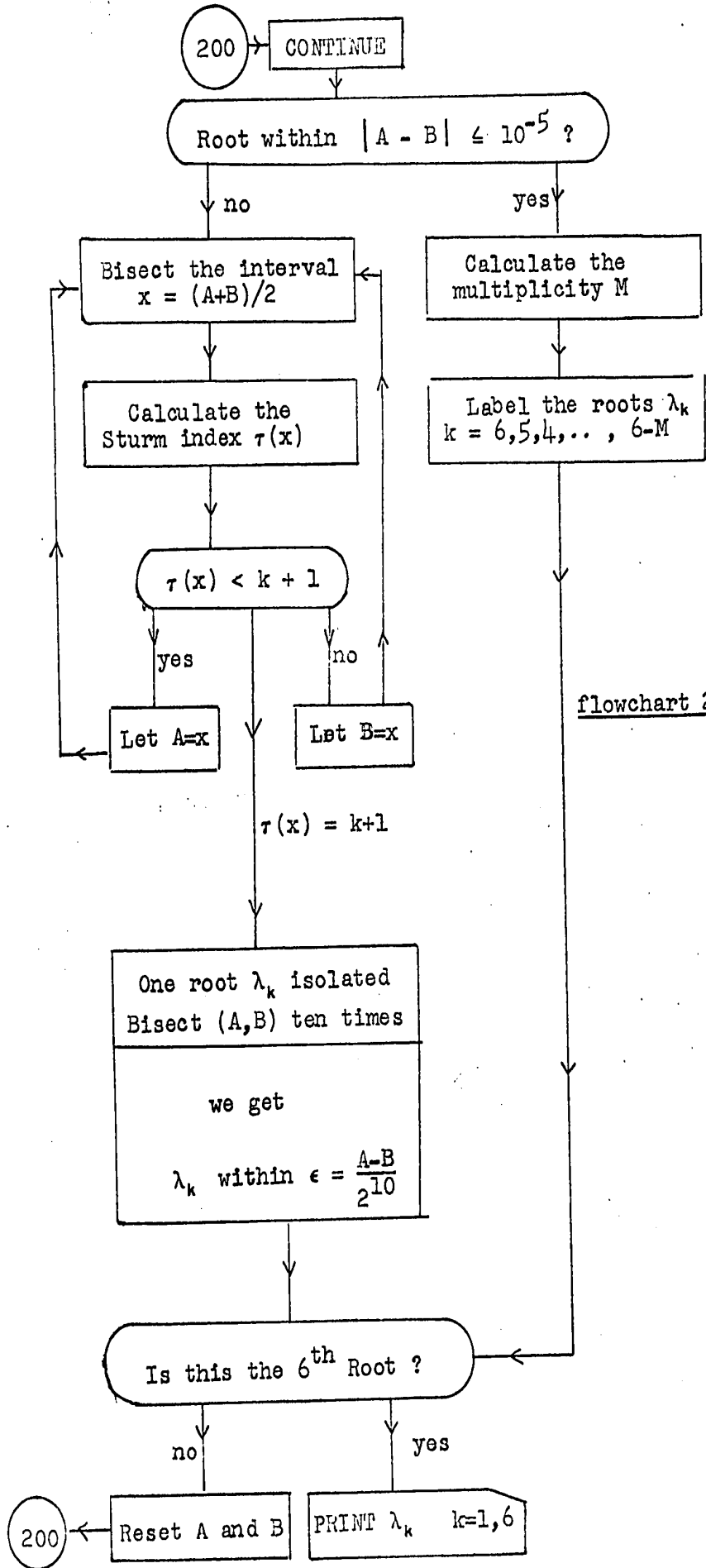
$$\mu = 1 / [2 b_{r,r+1} b_{r,r+1}^* \sqrt{1 + \chi^2} (\sqrt{1 + \chi^2} + 1)]$$

$$Y = BZ$$

$$q = Z' Y$$

$$= 2\mu (Y - \mu q Z)$$

$$\bar{B} = B - WZ' - ZW'$$



flowchart 2.

APPENDIX III

1) Kellermann Coefficients

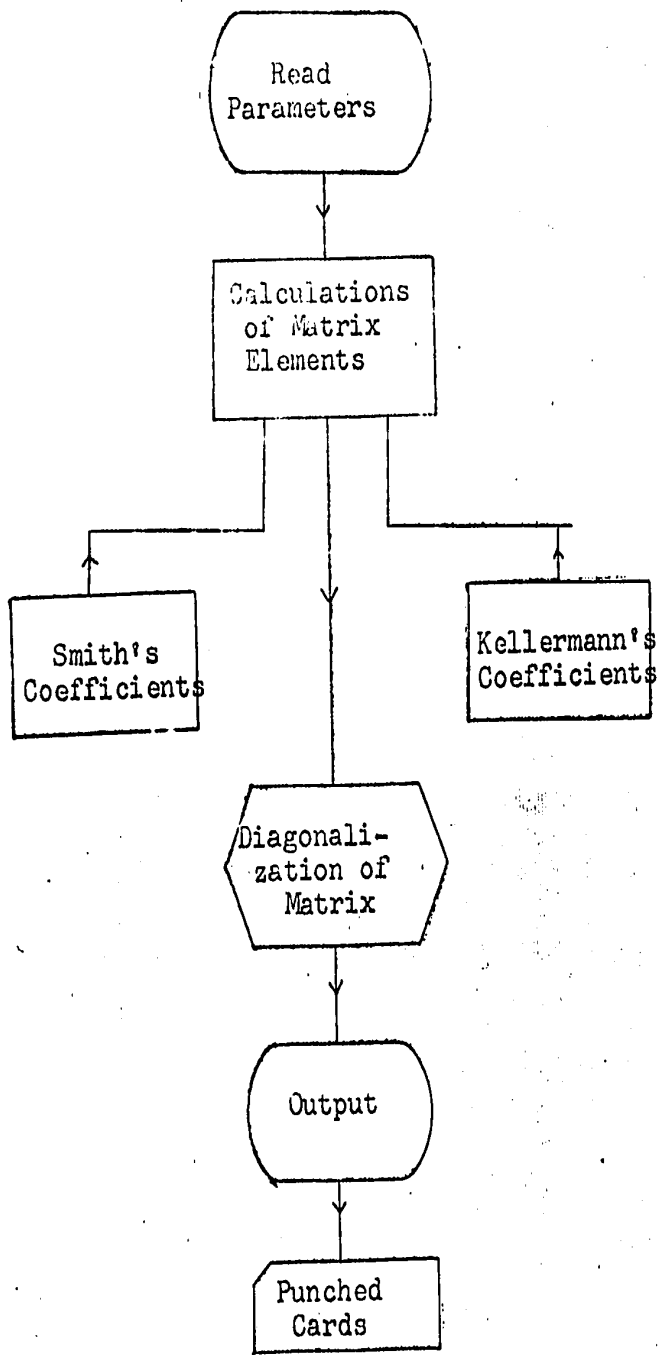
Various tests showed that for the choice of $\epsilon = 1$ the sums \sum_h , \sum_i and \sum_m have to be carried out using 35, 42, 109 terms respectively to obtain good accuracy. A program was written in which

$$\psi(l) = \int_0^l e^{-\xi^2} d\xi$$

was calculated by means of an approximation due to Hastings³⁷.

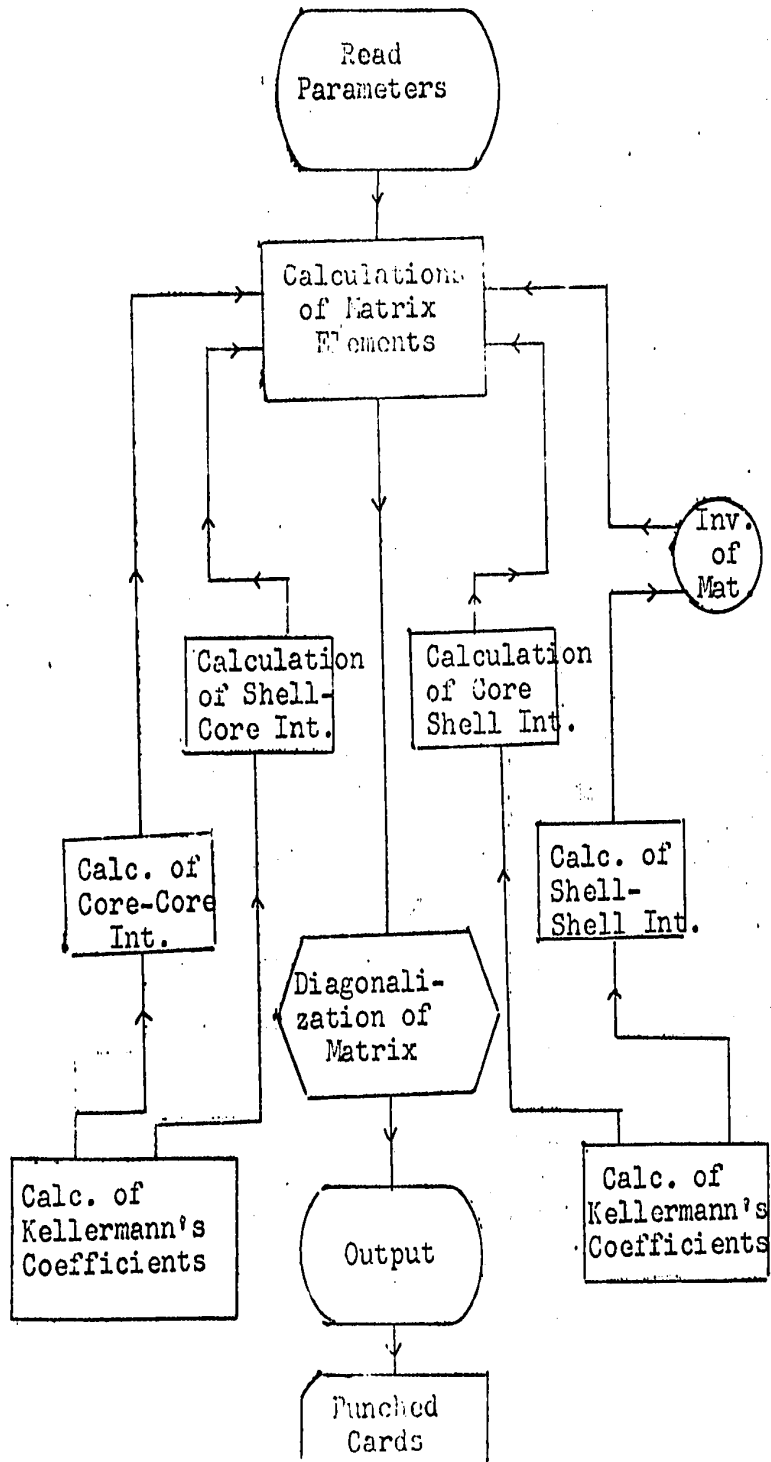
2) Calculations For SNI Model and KS Model

The parameters and other relevant data were fed in the computer and programming was done in the way shown in the flow chart. At the output, we obtained punched cards with different frequencies and their appropriate statistical weight. These frequencies were sorted and calculations were again carried out to obtain Debye temperature Θ_D .



Flow Chart III: SNI MODEL

Flow Chart IV



References

1. Welker, H.Z., Naturforsch, 7a, 744 (1952).
2. Welker, H.Z., Naturforsch, 8a, 248 (1953).
3. Madelung, O., Physics of III-V compounds (1964).
4. Born, M. and von Karman, Th., Phys. Z., 13, 297 (1912).
5. Born, M., Ann. Phy. Lpz. 44, 605 (1914).
6. Smith, H.M.J., Phil. Tran. Roy. Soc. Lond. A241, 105 (1948).
7. Nagendra Nath, N.S., Proc. Indian Acad. Sci. 1, 330 (1934).
8. Hsieh, Y.C., J. Chem. Phys. 22, 306 (1954).
9. Dayal, B. and Singh, S.P., Proc. Phys. Soc. 76, 777 (1960).
10. Brockhouse, B.N. and Iyengar, P.K., Phys. Rev. 111, 747 (1958).
11. Herman, F., J. Phys. Chem. Sol. 8, 405 (1959).
12. Pope, N.K., Lattice Dynamics Proceedings Int. nat. Conf. Copenhagen (1964) p. 147.

13. Braunstein, R., Herman, F. and Moore, A.R., Phys. Rev. 109, 695 (1958).
14. Dick, B.G. and Overhauser, A.W., Phys. Rev. 112, 90 (1958).
15. Cochran, W., Proc. Roy. Soc. A253, 260 (1959).
16. Woods, A.D.B., Cochran, W. and Brockhouse, B.N., Phys. Rev. 119, 980 (1960).
17. Cowley, R.A., Proc. Roy. Soc. A268, 109, 121 (1962).
18. Tolpygo, K.B., Fiz. Tverd. Tela 2, 2655 (1960)
[Translation Sovt. Phys. - Solid State 2, 2367 (1961)]
19. Tolpygo, K.B. and Mashkevich, V.S., Zh. Eksperm. i Teor. Fiz. 32, 520 (1957).
[Translation: Soviet Phys. - JETP 5, 435 (1957)]
20. Dolling, G. and Cowley, R.A., Proc. Phys. Soc. 88, 463 (1966).
21. Blanchard, R.C. and Varshni, Y.P., Phys. Rev., 159, 599 (1967).
22. Dolling, G., Inelastic Scattering of Neutrons in Solids and Liquids, Vol. II (Vienna: International Atomic Energy Agency) pp. 37
23. Potter, R.F., J. Phys. Chem. Soc. 3, 223 (1957).

24. Sirota, N.N. and Gololobov, E.M., Doklady, Acad. Nauk. SSSR 156, 1075 (1964).
[Translation - Soviet Phys. - Doklady 9, 477 (1964)]
25. Kellermann, E.W., Phil. Trans. A238, 513 (1940).
26. Merten, L., Z. Naturforsch A13, 662, 1067 (1958).
27. Srinivasan, R. and Rajagopal, A.K., Z. Physik 158, 471 (1960).
28. Tolpygo, K.B., Fiz. Tverd. Tela. 3, 943 (1961)
[Translation - Soviet Phys. - Solid State 3, 2367 (1961)]
29. Kaplan, H. and Sullivan, J.J., Phys. Rev. 130, 120 (1963).
30. Dolling, G. and Waugh, J.L.T., Phys. Rev. 132, 2410 (1963).
31. Born, M. and Begbie, G., Proc. Roy. Soc. A188, 179 (1947).
32. Born, M., Atomtheorie des festen Zustandes, Leipzig, Teubner (1923).
33. Blackman, R.C., Phil. Mag. 3, 831 (1958).
34. Blanchard, R.C., Thesis, Ottawa University, 1967.

35. Bishop, R.E.D., "The matrix analysis of vibrations".
36. Wilkinson, J.H., Comput. J. 3, 23 (1960).
37. Hastings, C., "Approximation for digital computers", Princeton University Press (1955).
38. Piesbergen, U., Z. Naturforschg. 18a, 141 (1963).
39. Morrison, J.A., Leadbetter, A.J. and Flubacher, P., Phil. Mag. 4, 273 (1959).
40. Ludwig, W., J. Phys. Chem. Soc. 4, 283 (1958).

Curriculum Vitae

Name: Ranjan Banerjee

Born: Dacca, Undivided India, 1942

Educated: St. Xaviers College, Calcutta 1960-62

Calcutta University 1962-64

Ottawa University 1965-67

Course: Physics

Degree: B.Sc. (Honours) 1962

M.Sc. 1964